

Advanced Aqueous-Phase Phosphoramidation Reactions for Effectively Synthesizing Peptide–Oligonucleotide Conjugates Trafficked into a Human Cell Line

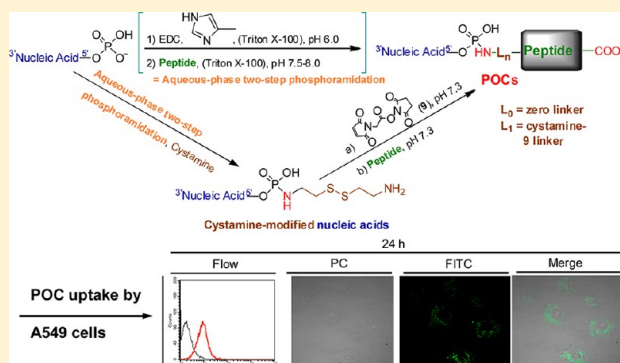
Tzu-Pin Wang,^{*,†} Ni Chien Ko,[†] Yu-Chih Su,[†] Eng-Chi Wang,[†] Scott Severance,[‡] Chi-Ching Hwang,[§] Ying Ting Shih,[⊥] Min Hui Wu,[†] and Yen-Hsu Chen^{*,⊥,||}

[†]Department of Medicinal and Applied Chemistry, [§]Department of Biochemistry, Faculty of Medicine, [⊥]School of Medicine, Graduate Institute of Medicine, College of Medicine, and ^{||}Division of Infectious Diseases, Department of Internal Medicine, Kaohsiung Medical University Hospital, Kaohsiung Medical University, Kaohsiung, 80708, Taiwan

[‡]Department of Science and Mathematics, Baptist Bible College, S. Abington Township, Pennsylvania 18411, United States

Supporting Information

ABSTRACT: Peptide–oligonucleotide conjugates (POCs) have held promise as effective therapeutic agents in treating microbial infections and human genetic diseases including cancers. In clinical applications, POCs are especially useful to circumvent cellular delivery and specificity problems of oligonucleotides. We previously reported that nucleic acid phosphoramidation reactions performed in aqueous solutions have the potential for facile POC synthesis. Here, we carried out further studies to significantly improve aqueous-phase two-step phosphoramidation reaction yield. Optimized reactions were employed to effectively synthesize POCs for delivery into human A549 cells. We achieved optimization of aqueous-phase two-step phosphoramidation reaction and improved reaction yield by (1) determining appropriate co-solutes and co-solute concentrations to acquire higher reaction yields, (2) exploring a different nucleophilicity of imidazole and its derivatives to stabilize essential nucleic acid phosphorimidazolide intermediates prior to POC formation, and (3) enhancing POC synthesis by increasing reactant nucleophilicity. The advanced two-step phosphoramidation reaction was exploited to effectively conjugate a well-studied cell penetrating peptide, the Tat_{48–57} peptide, with oligonucleotides, bridged by either no linkers or a disulfide-containing linker, to have the corresponding POC yields of 47–75%. Phosphoramidation-synthesized POCs showed no cytotoxicity to human A549 cells at studied POC concentrations after 24 h inoculation and were successfully trafficked into the human A549 cell line as demonstrated by flow cytometry, fluorescent microscopy, and confocal laser scanning microscopy study. The current report provides insight into aqueous-phase phosphoramidation reactions, the knowledge of which was used to develop effective strategies for synthesizing POCs with crucial applications including therapeutic agents for medicine.



INTRODUCTION

Extensive research endeavors have been devoted to exploring the therapeutic potential of nucleic acids, including siRNA, miRNA, catalytic RNA (ribozymes), aptamer oligonucleotides (oligonucleotides with exquisite roles similar to protein receptors), and antisense oligonucleotides.^{1–7} Theoretically, when designed appropriately, nucleic acids delivered into biological systems will participate in cellular activities, such as RNA interference or gene silencing, to abolish specific gene expression in cells and to attain more precise therapeutic targeting than typical small molecule drugs. Nucleic acid-based therapeutics have shown promise for treating a variety of human genetic diseases and microbial infections. Recent progress has resulted in some antisense oligonucleotides and aptamer RNA reaching clinical applications, while a significant number of clinical trials for siRNA are underway.^{1,3,5,6}

The direct use of nucleic acids for treating diseases, however, faces serious hurdles. Difficulties include cell specificity, inefficient cellular uptake of nucleic acids, and inaccessibility of nucleic acids to cell nuclei, due primarily to ineffective translocation of nucleic acids across biological barriers after administration.^{6,7} Consequently, successful use of nucleic acids in clinical practice will not be achieved until there are better strategies for targeted and efficient delivery of nucleic acids to cells and tissues.^{4–7} The critical issue of efficient target delivery for nucleic acids has been studied by many laboratories through chemical modification of nucleic acids to improve stability and cellular delivery properties of nucleic acids in vivo. Developed

Received: August 14, 2012

Revised: November 3, 2012

yl)-methyl]-carbamic Acid *tert*-Butyl Ester (**6a**). {2-[2-(2-*tert*-Butoxycarbonylamino-acetylamino)-acetylamino]-acetylamino}-acetic acid (**4**; 70 mg, 0.20 mmol) was first sonicated to completely dissolve in 20 mL DMF, followed by submerging the reaction mix in an ice–water bath. EDC (40 mg, 0.40 mmol) and HOBt (65 mg, 0.4 mmol) were then added to the reaction mixture to activate **4** for 15 min, followed by addition of a solution of mono-*t*-Boc-ethylenediamine (**5a**; 80 mg, 0.50 mmol) and DIPEA (0.035 mL, 0.40 mmol) in 5 mL of DMF to initiate the coupling reaction at rt for 6 h. Compound **5a** was previously synthesized according to similar reported procedures for **5b** synthesis.²⁰ The final reaction solution was filtrated, evaporated in vacuo, resuspended in 25% MeOH in DCM, and loaded to a silica column for further purification. The products were separated by eluting with mobile phases of 25% MeOH in DCM to afford **6a** (50 mg; 50%) as light yellowish solid. ¹H NMR (400 MHz) (DMSO-*d*₆) δ: 8.17 (t, 1H, CONHCH₂CH₂), 8.10–8.04 (m, 2H, Gly¹-NH, CH₂CH₂NH CO₂ C(CH₃)₃), 7.80 (t, 1H, Gly⁴-NH), 6.99 (t, 1H, Gly³-NH), 6.80 (t, 1H, Gly²-NH), 3.74 (t, 4H, Gly^{4α}-H, Gly^{1α}-H), 3.66 (d, 2H, Gly^{3α}-H), 3.58 (d, 2H, Gly^{2α}-H), 3.08 (q, 2H, NHCH₂), 2.98 (q, 2H, CH₂NH), 1.37 [d, 18H, CO₂C(CH₃)₃]. ¹³C NMR (DMSO-*d*₆) δ: 169.9, 169.4, 169.0, 168.8, 155.8, 155.6, 78.2, 77.7, 48.6, 43.3, 42.1, 42.1, 42.0, 40.1, 28.2, 28.2. HRMS (ESI) calculated for C₂₀H₃₆N₆O₈ Na, [M+Na]⁺ 511.2492 (calcd.), 511.2490 (found).

[6-(2-[2-(2-*tert*-Butoxycarbonylamino-acetylamino)-acetylamino]-acetylamino)-acetylamino]-hexyl]-carbamic Acid *tert*-Butyl Ester (**6b**). {2-[2-(2-*tert*-Butoxycarbonylamino-acetylamino)-acetylamino]-acetylamino}-acetic acid (**4**; 100 mg, 0.29 mmol) was first sonicated to completely dissolve in 20 mL DMF, followed by immersing the reaction mix in an ice–water bath. EDC (110 mg, 0.58 mmol) and HOBt (78 mg) were initially added to the reaction mix to activate **4** for 15 min, followed by addition of a solution of mono-*t*-Boc-hexanediamine (**5b**; 63 mg, 0.29 mmol)²⁰ and DIPEA (0.1 mL, 0.29 mmol) in 5 mL of DMF to commence the coupling reaction at rt for 6 h. The final reaction mixture was filtrated, evaporated in vacuo, redissolved in 10% MeOH in DCM, and loaded to a silica column for further purification. The products were separated by eluting with mobile phases of 10% MeOH in DCM to afford **6b** (85 mg; 54%) as a yellowish solid. ¹H NMR (400 MHz) (DMSO-*d*₆) δ: 8.16 (t, 1H, CONHCH₂CH₂), 8.04–8.08 [m, 2H, Gly⁴-NH, NH CO₂C(CH₃)₃], 7.70 (t, 1H, Gly³-NH), 7.00 (t, 1H, Gly¹-NH), 6.75 (t, 1H, Gly²-NH), 3.75 (d, 2H, Gly^{1α}-H), 3.72 (d, 2H, Gly^{4α}-H), 3.65 (d, 2H, Gly^{3α}-H), 3.58 (d, 2H, Gly^{2α}-H), 3.03 (q, 2H, NHCH₂), 2.88 (q, 2H, CH₂NH), 1.37 [d, 22H, CO₂C(CH₃)₃, NHCH₂CH₂], 1.21–1.23 (m, 4H, CH₂). ¹³C NMR (DMSO-*d*₆) δ: 169.9, 169.4, 169.0, 168.4, 155.9, 155.6, 78.2, 77.3, 43.3, 42.2, 42.1, 42.0, 38.9, 38.5, 29.5, 29.1, 28.3, 28.2, 26.1, 26.0. HRMS (ESI) calculated for C₂₄H₄₄N₆O₈ Na, [M+Na]⁺ 567.3118 (calcd.), 567.3115 (found).

2-Amino-N-[[[[(2-amino-ethylcarbamoyle)-methyl]-carbamoyle)-methyl]-carbamoyle)-methyl]-acetamide (**7a**). [[[[[(2-*tert*-Butoxycarbonylamino-ethylcarbamoyle)-methyl]-carbamoyle)-methyl]-carbamoyle)-methyl]-carbamoyle)-methyl]-carbamic acid *tert*-butyl ester (**6a**; 50 mg, 0.12 mmol) was dissolved in a TFA/DCM solution (1:1; 4 mL), stirred at 0 °C for 1 h, and then reacted at rt for 1 h. The product was evaporated under reduced pressure, washed by ether and chloroform, sequentially, and again concentrated under reduced pressure to remove ether and chloroform to give the yellow-

colored oil-like TFA salt of **7a**. The obtained TFA salt of **7a** was further dissolved in 5 mL of a DCM/MeOH mixture (DCM/MeOH = 1:1) and mixed with 10 equiv of Amberlyst A-21 (0.14 mg, 1.1 mmol) while rocking for 30 min.²⁰ After filtering to remove Amberlyst A-21, the filtrate of the reaction products was concentrated under reduced pressure to give white solid **7a** (30 mg, 95%). ¹H NMR (400 MHz) (DMSO-*d*₆) δ: 8.65 (t, 1H, NHCH₂CH₂), 8.32 (t, 1H, Gly⁴-NH), 8.17 (t, 1H, Gly³-NH), 8.06 (t, 1H, Gly²-NH), 7.80–8.02 (br, 4H, Gly¹-NH₂, CH₂CH₂NH₂), 3.85 (d, 2H, Gly^{4α}-H), 3.77 (d, 2H, Gly^{3α}-H), 3.71 (d, 2H, Gly^{2α}-H), 3.62 (s, 2H, Gly^{1α}-H), 3.30 (q, 2H, CH₂NH), 2.85 (q, 2H, NHCH₂). ¹³C NMR (DMSO-*d*₆) δ: 169.6, 169.1, 168.8, 166.4, 42.0, 42.0, 42.0, 39.0, 38.5, 36.3. HRMS (ESI) calculated for C₁₀H₂₁N₆O₄, [M+H]⁺ 289.1624 (calcd.), 289.1626 (found).

2-Amino-N-[[[[(6-amino-hexylcarbamoyle)-methyl]-carbamoyle)-methyl]-carbamoyle)-methyl]-acetamide (**7b**). [6-(2-[2-(2-*tert*-Butoxycarbonylamino-acetylamino)-acetylamino]-acetylamino)-hexyl]-carbamic acid *tert*-butyl ester (**6b**; 60 mg, 0.11 mmol) was dissolved in a TFA/DCM solution (1:1; 4 mL), stirred at 0 °C for 1 h, and then reacted at rt for 1 h. The product was evaporated under reduced pressure, washed by ether and chloroform, sequentially, and again concentrated under reduced pressure to remove ether and chloroform to obtain the brown oil-like TFA salt of **7b**. The acquired TFA salt of **7b** (0.52 g, 0.88 mmol) was further dissolved in 5 mL of DCM/MeOH mixture (DCM/MeOH = 1:1) and mixed with 10 equiv of Amberlyst A-21 (0.14 mg, 1.1 mmol) while rocking for 30 min.²⁰ After filtering to remove Amberlyst A-21, the filtrate of the reaction products was concentrated under reduced pressure to afford white solid **7b** (50 mg, 95%). ¹H NMR (400 MHz) (DMSO-*d*₆) δ: 8.68 (t, 1H, NHCH₂CH₂), 8.33 (t, 1H, Gly⁴-NH), 8.13 (t, 1H, Gly³-NH), 7.84–8.08 (br, 4H, Gly¹-NH₂, CH₂CH₂NH₂), 7.79 (t, 1H, Gly²-NH), 3.84 (d, 2H, Gly^{4α}-H), 3.75 (d, 2H, Gly^{3α}-H), 3.66 (d, 2H, Gly^{2α}-H), 3.62 (s, 2H, Gly^{1α}-H), 3.04 (q, 2H, CH₂NH), 2.76 (t, 2H, CH₂NH₂), 1.18–1.60 (m, 8H, CH₂). ¹³C NMR (DMSO-*d*₆) δ: 169.0, 168.9, 168.5, 166.5, 42.1, 42.5, 42.0, 40.2, 38.8, 38.4, 28.9, 27.0, 25.8, 25.5. HRMS (ESI) calculated for C₁₄H₂₉N₆O₄, [M+H]⁺ 345.2250 (calcd.), 345.2251 (found).

Synthesis of a N-Maleoyl Amino Acid Succinimidyl Ester, AMAS (9). (2,5-Dioxo-2,5-dihydro-pyrrol-1-yl)-acetic acid 2,5-dioxo-pyrrolidin-1-yl ester (**9**) was synthesized from (2,5-dioxo-2,5-dihydro-pyrrol-1-yl)-acetic acid (**8**) which was prepared by a previously reported method.²² The acquired **8** (69 mg, 0.45 mmol) and NHS (103 mg, 0.89 mmol) were first dissolved in THF (10 mL), followed by dropwise addition of DCC (184 mg, 0.89 mmol) in THF (10 mL) while stirring. After overnight reaction at rt, the mixture was quenched by addition of three drops of glacial acetic acid and stirring for 1 h and filtered to remove suspension. The acquired filtrate was concentrated under reduced pressure, washed by EtOH twice, resuspended in 2-propanol (30 mL) while stirring for 1 h, and filtered to separate the suspension from its filtrate. The final solid was washed by 2-propanol and dried to afford a white-colored **9** (96 mg; 86%). ¹H NMR (400 MHz) (DMSO-*d*₆) δ: 7.20 (s, 2H, CHCH), 4.73 (s, 2H, CH₂), 2.81 (s, 4H, CH₂CH₂) ¹³C NMR (DMSO-*d*₆) δ: 169.7, 169.7, 164.4, 135.1, 36.3, 25.4. HRMS (ESI) calculated for C₁₀H₈N₂O₆Na, [M+Na]⁺ 275.0280 (calcd.), 275.0279 (found).

Synthesis of the Thiol-Containing Biotin Derivative (13). 5-(2-Oxo-hexahydro-thieno[3,4-*d*]imidazol-4-yl)-penta-noic acid (2-[2-[5-(2-oxo-hexahydro-thieno[3,4-*d*]imidazol-

4-yl)-pentanoylamino]-ethylidisulfanyl]-ethyl)-amide (12). 5-(2-Oxo-hexahydro-thieno[3,4-*d*]imidazol-4-yl)-pentanoic acid 2,5-dioxo-pyrrolidin-1-yl ester (11; 0.19 g, 0.55 mmol) was synthesized from 10 according to our previously published method²⁰ and was completely dissolved in DMF (7 mL) with gentle warming. After slowly cooling the 11 solution to rt without recurring precipitation, it was mixed with an aqueous solution (1 mL) containing cystamine dihydrochloride (0.068 g, 0.30 mmol) and Et₃N (0.14 g, 1.38 mmol) with stirring. The reaction proceeded at rt overnight with stirring and the reaction products were concentrated in vacuo. The remaining solid was redissolved in 2-propanol (20 mL) with gentle heating, cooled down to room temperature, and reprecipitated at 4 °C overnight. The obtained white solid was recovered from the glassware, washed with cold 2-propanol and air-dried to give 12 (0.14 g; 82.1%). ¹H NMR (400 MHz) (DMSO) δ: 8.01 (s, 2H, CONH), 6.54 (s, 2H, CONH), 6.39 (s, 2H, CONH), 4.31 (t, 2H, CHN), 4.15 (t, 2H, CHN), 3.11 (dd, 2H, CHS), 2.85 (d, 2H, CHHS), 2.78 (t, 4H, CH₂S), 2.58 (d, 2H, CHHS), 2.09 (t, 4H, CH₂CO), 1.31–1.61 (m, 12H). ¹³C NMR (100.67 MHz) (DMSO) δ: 172.26, 162.74, 61.04, 59.21, 55.43, 41.10, 37.88, 37.31, 35.15, 28.11, 25.23. HRMS (ESI) calculated for C₂₄H₄₀N₆O₄S₄Na, [M+Na]⁺ 627.1891 (calcd.), 627.1893 (found).

5-(2-Oxo-hexahydro-thieno[3,4-*d*]imidazol-4-yl)-pentanoic acid (2-mercapto-ethyl)-amide (13). 5-(2-Oxo-hexahydro-thieno[3,4-*d*]imidazol-4-yl)-pentanoic acid (2-{2-[5-(2-oxo-hexahydro-thieno[3,4-*d*]imidazol-4-yl)-pentanoylamino]-ethylidisulfanyl]-ethyl)-amide (12; 0.14 g, 0.23 mmol) was completely dissolved in DMF (8 mL) with gentle warming. After cooling, the 12 solution to rt without recurring precipitation, DL-dithiothreitol (DTT; 0.11 g, 0.68 mmol) and Et₃N (0.002 g, 0.02 mmol) were added to the solution with stirring. Additional DTT (0.11 g, 0.68 mmol) was replenished to the reaction mixture 1 h later. The reaction proceeded at rt for 2 more hours, followed by evaporation in vacuo. The remaining solid was washed by DCM (10 mL) three times and concentrated under reduced pressure to give white-colored 13 (0.07 g; 52.7%). ¹H NMR (400 MHz) (DMSO) δ: 7.98 (s, 1H, CONH), 6.45 (s, 1H, CONH), 6.38 (s, 1H, CONH), 4.32 (t, 1H, CHN), 4.14 (t, 1H, CHN), 3.19 (t, 2H, CH₂SH), 3.11 (dd, 1H, CHS), 2.83 (d, 1H, CHHS), 2.58 (d, 1H, CHHS), 2.37 (t, 1H, SH), 1.32–1.61 (m, 6H). ¹³C NMR (100.67 MHz) (DMSO) δ: 172.38, 162.81, 61.07, 59.23, 55.44, 42.04, 35.14, 28.21, 28.03, 25.25, 23.52. HRMS (FAB) calculated for C₁₇H₃₀O₅N₅SNa, [M+Na]⁺ 439.5112 (calcd.), 439.1865 (found).

Nucleic Acid Preparation and Radiolabeling. The 3' primer (5'-TACCCCTTGGGGATACCACC-3'), a single-stranded DNA, was purchased from Purigo Biotech, Inc., Taiwan, and used without purification. The TW17₁₋₁₇ RNA (5'-GGGAUCGUCAGUGCAUU-3') was purchased from Bioneer (Daejeon, South Korea) and also used without purification. The 5' GMP-primed TW17 RNA (87-mer; 5'-GGGAUCGUCAGUGCAUUAGAGAAGUGCAGUGUCUUGCGCUGGGUUCGAGCGGUCCGUGGUGCUGGCCCGGUGGUAUCCCAAGGGGUA-3') was prepared as previously described.²³ The TW17 RNA body-labeled with ³²P and the 3' primer DNA ³²P-labeled at the 5'-end were prepared according to the previously reported procedures.^{20,23}

Optimization of Two-Step Nucleic Acid Phosphoramidation Reactions. The optimized two-step phosphoramidation reaction for RNA was carried out by dissolving the

GMP-primed TW17 RNA (0.32 nmol) and EDC (4.17 μmol) in 4 μL 4(5)-methylimidazole-Triton X-100 buffer [0.1 M 4(5)-methylimidazole, 15% Triton X-100, pH 6.0] and activating at rt for 90 min. The resulting 5'-phosphorimidazolide RNA was purified by ethanol precipitation and resuspended in 5.5 μL of EPPS-Triton X-100 buffer (100 mM EPPS, 15% Triton X-100, 2 mM EDTA, pH 7.5). One microliter of 1 (187.2 mM in DMF) was then added to the 5'-phosphorimidazolide RNA solution to allow a phosphoramidation reaction at 41 °C for 3 h.

For the single-stranded 3'-primer DNA, the optimized two-step phosphoramidation reaction was performed by dissolving the single-stranded DNA (0.32 nmol) and EDC (4.17 μmol) in 4 μL of 4(5)-methylimidazole buffer [0.1 M 4(5)-methylimidazole, pH 6.0] and activating at rt for 90 min. Similarly, the resulting 5'-phosphorimidazolide DNA was purified by ethanol precipitation and redissolved in 5.5 μL of EPPS buffer (100 mM EPPS, 2 mM EDTA, pH 7.5). A solution of 1 (1 μL; 187.2 mM in DMF) was later added to the 5'-phosphorimidazolide DNA solution to allow a phosphoramidation reaction at 55 °C for 3 h. No co-solute was used in the two-step phosphoramidation reaction of the single-stranded DNA to attain higher reaction yield.

All resulting nucleic acid–substrate conjugates were purified twice by ethanol precipitation, analyzed by urea-PAGE and SA gel shift assay (8% urea-PAGE for the TW17 RNA, and 20% urea-PAGE for single-stranded DNA), visualized, and quantified by an Amersham Typhoon PhosphorImager to determine reaction yield.

Nucleic Acid-Tetraglycine Derivative Conjugate Preparation. The phosphoramidation reactions between the TW17 RNA and 6a/6b adhered to the optimized two-step phosphoramidation reaction stated above but with 1 replaced by the same concentration of 6a/6b. The phosphoramidation reactions between the 3' primer DNA and 6a/6b was also carried out by following the previously optimized two-step phosphoramidation reaction for single-stranded DNA but with the same concentration of 6a/6b substituting for 1. The synthesized nucleic acid-tetraglycine derivative conjugates were purified twice by ethanol precipitation, analyzed by 8% (the TW17 RNA) or 20% (the 3' primer DNA) urea-PAGE to separate reaction products, visualized and quantified by an Amersham Typhoon PhosphorImager.

Two-Step Phosphoramidation Reactions for Synthesis of Nucleic Acid–Tat₄₈₋₅₇ Peptide Conjugates. The single-stranded 3'-primer DNA was conjugated with the Tat₄₈₋₅₇ peptide according to the optimized two-step phosphoramidation reaction described previously but with the following modifications. First, the scale of the reaction was increased five times to acquire the sufficient conjugates for subsequent ex vivo studies. In addition, the pH of the conjugation reaction between the 5'-phosphorimidazolide DNA and the Tat₄₈₋₅₇ peptide was increased to 8.0 achieved by addition of concentrated EPPS buffer (600 mM EPPS, 5 mM EDTA, pH 8.0) to attain higher yield. Finally, only 20 mM of the Tat₄₈₋₅₇ peptide was required in the coupling reaction to have the best yield.

For RNA-Tat₄₈₋₅₇ conjugates, preparation also followed the optimized two-step RNA phosphoramidation reaction but with following modifications: (1) Only 20 mM of the Tat₄₈₋₅₇ peptide was required in conjugation reactions, and (2) concentrated EPPS-Triton X-100 buffer (600 mM EPPS, 15% Triton X-100, 5 mM EDTA, pH 7.5) was added to the

conjugation reaction between the 5'-phosphorimidazole RNA and the Tat_{48–57} peptide to retain the buffering capacity.

The synthesized nucleic acid-Tat_{48–57} conjugates were also purified twice by ethanol precipitation, analyzed by 8% (the TW17 RNA) or 20% (the 3' primer DNA and the TW17_{1–17} RNA) urea-PAGE, visualized and quantified by an Amersham Typhoon PhosphorImager.

Two-Step Phosphoramidation Reactions for Synthesis of Nucleic Acid–Cystamine Conjugates. Similar optimized two-step phosphoramidation reactions were applied when preparing nucleic acid–cystamine conjugates and are described below. The RNA–cystamine conjugate synthesis was carried out by dissolving the GMP-primed TW17_{1–17} RNA (0.32 nmol) and EDC (4.17 μ mol) in 4 μ L of 4(5)-methylimidazole-Triton X-100 buffer and activating at rt for 90 min. The resulting 5'-phosphorimidazole RNA was purified by ethanol precipitation and then resuspended in 5.5 μ L of concentrated EPPS-Triton X-100 buffer with the addition of 1 μ L of cystamine (187.2 mM in water) to allow a reaction at 41 °C for 3 h.

For the single-stranded 3'-primer DNA, the cystamine conjugate was prepared by dissolving the DNA (1.59 nmol) and EDC (26 μ mol) in 20 μ L 4(5)-methylimidazole buffer and activating at rt for 90 min. The resulting 5'-phosphorimidazole DNA was purified by ethanol precipitation, redissolved in 27.5 μ L of concentrated EPPS buffer. Five microliters of cystamine (187.2 mM in DEPC water) was then added to the 5'-phosphorimidazole DNA solution to allow reaction at 55 °C for 3 h. Again, no co-solute was used in the two-step phosphoramidation reaction of the single-stranded DNA to attain higher reaction yield.

The products of the conjugation reactions between cystamine and nucleic acids were separated by 20% urea-PAGE, visualized and quantified by an Amersham Typhoon PhosphorImager to determine reaction yield.

Optimization of AMAS (9) Reactions to Effectively Conjugate Nucleic Acids with the C(KFF)₃K Peptide. The heterobifunctional 9 served as the linker to conjugate cystamine-modified nucleic acids with peptides (Scheme S1). Before having 9 react with cystamine-modified nucleic acids and peptides, each reaction was optimized by using one of the model compounds 11 and 13 to attain the highest yield. The optimization reactions are briefly described below.

For the reaction between a cystamine-modified nucleic acid and 9, 11 with an activated carboxyl group was substituted for 9. The substitution simplified the acylation reaction allowing the determination of the appropriate condition to provide the highest yield as stated below. The cystamine-modified 3' primer DNA (900 pmol) was dissolved in 22.5 μ L of concentrated EPPS-7.3 buffer (600 mM EPPS, pH 7.3) to produce 40 μ M of the DNA solution in a microfuge tube. After addition of 11 solution (9 μ L; 0.01–1 M in DMF), the microfuge tube was wrapped with aluminum foil, and reacted at rt with rocking for 1.5 h. The resulting 3' primer DNA-11 conjugates were purified twice by ethanol precipitation, analyzed by 20% urea-PAGE, visualized and quantified by an Amersham Typhoon PhosphorImager to determine reaction yield.

The conjugation of the 9-modified 3' primer DNA with 13 was studied to determine optimal conditions for the Michael addition reaction between the 9-modified nucleic acids and cysteine-containing peptides and to attain high yield (Scheme S1; Supporting Information). The reaction optimization is briefly described below. Assuming no DNA loss during ethanol

precipitation, the acquired 9-modified 3' primer DNA reaction mixture (0.9 nmol) was dissolved in 50 μ L of concentrated EPPS-7.3 buffer, followed by the slow addition of 50 μ L of 13 solution (36–3600 μ M in DMF), and reacted at rt with rocking for 16 h. The acquired 3' primer DNA-13 conjugates were purified twice by ethanol precipitation, analyzed by 20% urea-PAGE, visualized and quantified by an Amersham Typhoon PhosphorImager to determine reaction yield.

Synthesis of Nucleic Acid–C(KFF)₃K Peptide Conjugates Using the Cystamine-9 Linker. All nucleic acid–C(KFF)₃K peptide conjugates were prepared by following the optimized AMAS (9) reactions described previously and briefly stated below. The TW17_{1–17} RNA–C(KFF)₃K peptide conjugate synthesis was initiated by dissolving the previously prepared cystamine-modified TW17_{1–17} RNA (0.22 nmol) in 5.55 μ L of concentrated EPPS-7.3 buffer to yield a 40 μ M RNA solution. After addition of 22 μ L of 9 (10 mM in DMSO) to the RNA solution, the microfuge tube containing the RNA reaction mixture was wrapped with aluminum foil and reacted at rt with rocking for 1.5 h. The 9-modified RNA was purified by standard ethanol precipitation to remove excess 9, and was redissolved in 50 μ L of concentrated EPPS-7.3 buffer. A solution of C(KFF)₃K solution (50 μ L; 4.4 nmol) was then slowly added to the 9-modified RNA solution and reacted at rt with rocking for 16 h (Scheme S1).

For DNA conjugates, the cystamine-modified 3' primer DNA (0.9 nmol) was dissolved in 22.5 μ L of concentrated EPPS-7.3 buffer to produce a 40 μ M DNA solution in a microfuge tube. A solution of 9 (90 μ L; 10 mM in DMSO) was added to the DNA solution and followed by wrapping the reaction mixture-containing microfuge tube with aluminum foil and rocking the reaction mixture at rt for 1.5 h. The reaction products were purified twice by ethanol precipitation to remove excess 9. The obtained 9-modified 3' primer DNA (~0.9 nmol) was redissolved in 50 μ L of concentrated EPPS-7.3 buffer, followed by slow addition of 50 μ L of the C(KFF)₃K peptide solution (18 nmol in DEPC water), and reacted at rt with rocking for 16 h (Scheme S1). The obtained nucleic acid–C(KFF)₃K peptide conjugate was purified twice by ethanol precipitation, analyzed by 20% urea-PAGE, visualized and quantified by an Amersham Typhoon PhosphorImager to obtain reaction yield.

MALDI-TOF MS for POC Characterizations. Prior to MALDI-TOF analysis, each POC sample was purified by urea-PAGE and desalted by passing through a Sephadex G-10 (GE Healthcare Life Sciences, Taipei, Taiwan). MALDI-TOF mass spectra were recorded on an Autoflex III TOF/TOF analyzer (Bruker Daltonics, Taiwan). Each MALDI-TOF sample was prepared by mixing a purified POC (100 pmol in 0.5 μ L water) with the MALDI-TOF matrix solution (0.5 μ L), deposited on a target plate and allowed to dry before the POC mass measurement. A fresh MALDI-TOF matrix solution was prepared daily by adopting a volume ratio of 1:2:1 for 2,3,4-trihydroxyacetophenone (0.2 M in 50% acetonitrile), 2,4,6-trihydroxyacetophenone (0.2 M in 50% acetonitrile), and ammonium citrate (0.3 M), respectively.

Cell Culture. Cells of A549, a human lung carcinoma cell line, were maintained in Ham's F12K (Biowest, France) and supplemented with 10% fetal bovine serum (FBS; Hyclone, USA), 1% penicillin–streptomycin–amphotericin (PSA; Biological Industries, Israel), and 1% L-glutamine solution (Biological Industries, Israel).

Cytotoxicity Assays. The viability of mammalian cells in the presence of POCs was determined by the methylthiazole-

trazolium (MTT) conversion assay described previously.²⁴ A549 cells were cultured in 96 well plates (2×10^4 cells/well; 0.1 mL medium/well), washed, and maintained in medium containing serum overnight prior to assay. After inoculation with 0–10 μM of the 3' primer, DNA- Tat_{48–57} peptide conjugate, cells were maintained at 37 °C for 24 h and further incubated with MTT (0.5 mg/mL) at 37 °C for 4 h. By the end of MTT incubation, the medium was removed and the insoluble formazan product was dissolved by adding DMSO (100 μL /well) with thoroughly mixing. MTT conversion was determined by colorimetric analysis at 570 nm. Each experiment was performed in triplicate; the reported result was mean of triplicate experiments \pm SD.

Fluorescent Labeling of DNA and Its Conjugation with the Tat_{48–57} Peptide. In order to detect the uptake of DNA in POCs by mammalian cells using flow cytometry, fluorescent microscopy, and confocal laser scanning microscopy, the DNA was required to be labeled with fluorophores before conjugating with the Tat_{48–57} peptide for POC synthesis. Fluorescent labeling of DNA was achieved by a DNA depurination method²⁵ and briefly described below. DNA depurination was accomplished by resuspension of the 3' primer DNA (1–10 mg) in 0.2 N HCl (10 mL) and allowed to react at 37 °C for 90 min. The depurinated DNA solution was diluted with 40 mL of ethylenediamine buffer (650 mM, pH 7.6) and reacted at 37 °C for 3 h. The solution of the imine-containing DNA was further reacted with freshly prepared NaBH₄ (0.1 M in water, 4 mL) at rt for 30 min. The acquired diamino-derivatized DNA sample was purified by adding 1 mL of lithium perchlorate (2% in acetone) to precipitate the DNA, washing the DNA with acetone twice and air-drying. After redissolving the diamino-derivatized DNA in carbonate buffer (0.1 M, pH 9.0; 20 μL), a solution of fluorescein isothiocyanate (FITC; 2.57 mM in DMSO, 20 μL) was slowly added to the DNA solution and reacted in the dark for 12 h. The reaction products were precipitated by ethanol and further purified by 20% urea-PAGE to obtain the FITC-labeled 3' primer DNA. The FITC-labeled DNA was conjugated with the Tat_{48–57} peptide according to the optimized zero-linker two-step phosphoramidation reaction described in this study. The POC, the FITC-labeled 3' primer DNA- Tat_{48–57} peptide conjugate, was again purified by 20% urea-PAGE in which the migration of the FITC-labeled POC was visualized by an Amersham Typhoon PhosphorImager with the settings of the excitation wavelength at 488 nm and the emission wavelength at 525 nm for fluorescein detection. It is noted that the FITC-labeled Tat_{48–57} peptide was also prepared according to a previously described method.²⁰

Flow Cytometry. A549 cells were seeded into a 12-well plate (2×10^5 cells in 1 mL medium per well) and cultured overnight. The medium in the overnight cultures was removed, replenished with a fresh medium containing 0 or 5 μM of the FITC-labeled Tat_{48–57} peptide or 3' primer DNA–Tat_{48–57} peptide conjugate, and further maintained at 37 °C for 24 h. The peptide/POC-containing medium was discarded after incubation in which the cells were washed by PBS once and detached from the plate surface by treating with trypsin (trypsin–EDTA 1 \times , 0.5 mL per well; Biowest, France) for 3–5 min. The trypsinized cells were resuspended in the medium (0.5 mL) and centrifuged at 700 rcf for 4 min. After removal of the supernatants, the cells were resuspended in ice-cold PBS (1 mL) and subjected to another round of centrifugation (700 rcf for 4 min). The final cell pellets were again resuspended in ice-

cold PBS (1 mL), transferred to Falcon tubes (BD Bioscience, San Jose, CA, USA) and placed on ice in the dark before each analysis. Each experiment was performed in triplicate; in each case, the fluorescence of at least 10 000 viable cells was measured by using a BD FACSCalibur cytometer (BD, Franklin Lakes, NJ, USA).

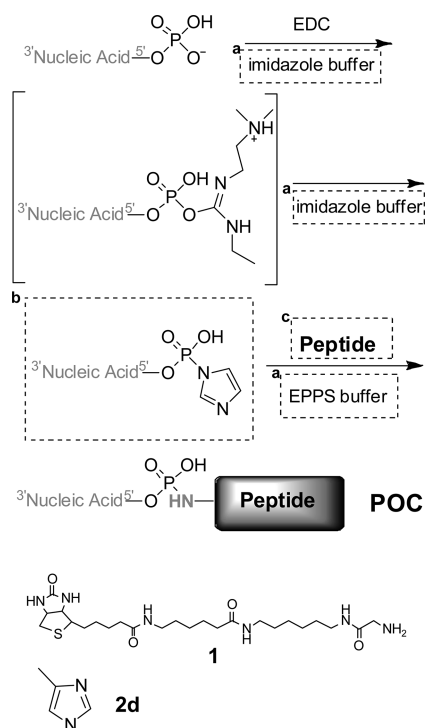
Confocal Laser Scanning Microscopy and Fluorescent Microscopy. A549 cells were seeded in an 8-well Lab-Tek coverglass chamber (0.3 mL medium per well; Nalge Nunc, Rochester, NY, USA) with an appropriate density of 1×10^4 cells per well and incubated for 24 h before the experiment. The medium in the overnight cultures was removed, replenished with a fresh medium containing 0 or 5 μM of the FITC-labeled Tat_{48–57} peptide or 3' primer DNA–Tat_{48–57} peptide conjugate, and further maintained at 37 °C for 24 h. The peptide/POC-containing medium was discarded after incubation, followed by washing the cells with PBS three times before confocal imaging analysis. The pictures were obtained using a FluoView 1000 confocal laser scanning microscope (Olympus, Tokyo, Japan). All images were acquired using living and nonfixed cells. Each experiment was performed in triplicate. Experimental procedures similar to those described above were used in fluorescent microscopy analysis.

RESULTS

General Considerations in Optimizing the Aqueous-Phase Two-Step Phosphoramidation Reactions for POC Synthesis. We envisioned that three aspects of two-step nucleic acid phosphoramidation reactions critical to POC synthesis could be modified to increase product yields (Scheme 1). First, inert co-solutes such as Tween 20 and Triton X-100 were substituted for urea (8 M in the original reactions)²⁰ in phosphoramidation reactions to ensure co-solutes would carry out their proposed roles of denaturing nucleic acids without participating in nucleophilic substitution reactions. Our previous study has revealed that using urea as a co-solute could lead to less than optimal reaction yield. Second, we sought to attain higher POC yields by modestly increasing the nucleophilicity of the imidazole moiety. Appropriately stabilizing phosphorimidazolide intermediates would extend their half-lives in aqueous solutions while not deterring subsequent nucleophilic substitution reaction with peptides. Third, POC yields could be further improved by chemically modifying peptides to increase peptide nucleophilicity. We adopted these three strategies to improve the aqueous-phase two-step phosphoramidation reactions and present the results in the following sections.

Identification of an Appropriate Co-Solute and Concentration to Facilitate POC Synthesis. We exploited previously synthesized **1** (Scheme 1) as the nucleophile in aqueous-phase two-step phosphoramidation reactions to optimize conjugation with nucleic acids. First, we substituted one of five different co-solutes (Triton X-100, Tween 20, PEG-6000, PEG-8000, and glycerol) for urea in the phosphoramidation reactions while varying co-solute concentrations from 0% to 33% (w/v) to identify appropriate co-solutes and concentrations for DNA and RNA conjugation with the nucleophile **1**. These co-solutes were chosen because each of their structures only contains the hydroxyl functionality, which is unlikely to deprotonate and participate in phosphoramidation reactions as nucleophiles at neutral pH. The TW17 RNA (87-mer nt) clearly favored 15% Triton X-100 in the phosphoramidation reactions to have the best yield (Figure 1A). The 3'

Scheme 1. Strategies to Optimize Aqueous-Phase Two-Step Phosphoramidation Reactions for Conjugating Nucleic Acid with Nucleophiles, Such as Peptides, to Synthesize Peptide–Oligonucleotide Conjugates (POCs)^a



^aDashed boxes indicate the approaches to improve the reaction yields. Each bold, superscripted, lower-case letter represents the specific method to explore reaction conditions to achieve best reaction yields. These methods include the following: a, identifying an appropriate cosolute and concentration; b, investigating imidazole derivatives to stabilize phosphorimidazolide intermediates and facilitate subsequent phosphoramidation reactions; c, increasing numbers of nucleophilic functionalities in nucleophiles which were peptides in this study. Compound **1** was one of the model nucleophiles in this study. Compound **2d** was identified as the best imidazole derivative for POC synthesis revealed by the results noted in the text.

primer DNA (20-mer nt), however, had the best yield when no co-solutes were included in the phosphoramidation reactions (Figure 1B). Acquiring better yield with no co-solutes in DNA phosphoramidation reactions is consistent with previous findings²⁰ and likely reflects short single-stranded DNA, such as the 3' primer DNA, having less of a tendency to fold into secondary structures which would interfere in phosphoramidation reactions. Having co-solute concentrations higher than 32.5% in two-step phosphoramidation reactions might promote product formation as implicated in Figure 1B, but this is an impractical approach as reaction mixtures became too thick to handle.

Survey of Imidazole Derivatives with Potential to Enhancing POC Formation. After determining optimal cosolute conditions in the two-step phosphoramidation reactions for nucleic acids, we substituted one of six imidazole derivatives (**2a–f**; Figure S1) for imidazole in reactions. All the imidazole derivatives have electron-donating substitutions in the aromatic ring which presumably strengthens phosphoramidate bonds and improves stability of the key phosphorimidazolide intermediates in water (boxed in **b** in Scheme 1). Results of the studied two-step phosphoramidation reactions in the

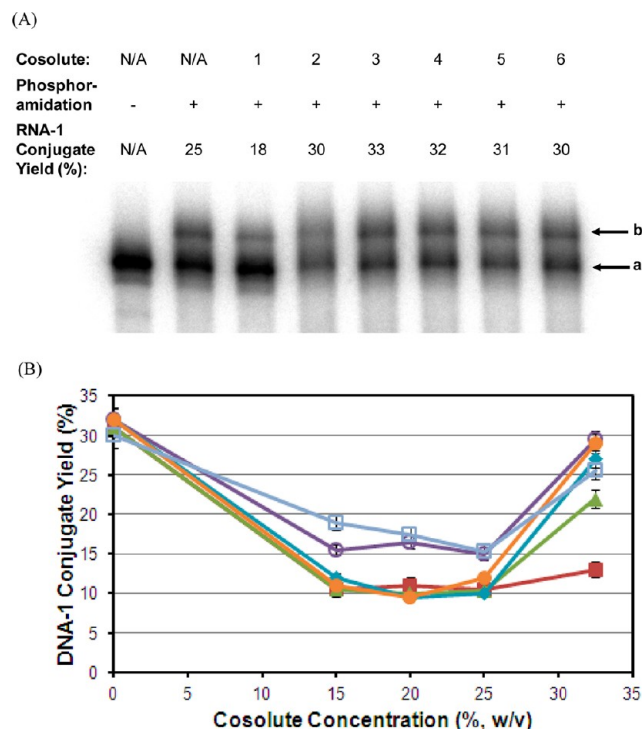


Figure 1. Effects of co-solutes on yields of aqueous-phase two-step phosphoramidation reactions when conjugating **1** with (A) the ³²P-labeled TW17 RNA or (B) the ³²P-labeled single-stranded 3' primer DNA. (A) The studied co-solutes included the following: 1, urea; 2, Tween 20; 3, Triton X-100; 4, PEG 6000; 5, PEG 8000; 6, glycerol. Each co-solute had a concentration of 15% (w/v) in both buffers for the phosphoramidation reactions. The reaction products were purified by ethanol precipitation, analyzed by 8% urea-PAGE, visualized and quantified by an Amersham Typhoon PhosphorImager. a, unreacted TW17 RNA; b, TW17 RNA-1 conjugate. (B) The relationship of cosolute concentrations and DNA-1 conjugate yields for each studied cosolute. The data were quantified by results from several urea-PAGE analyses similar to that in (A). Each data point is determined by calculating the average of the yields from triplicate experiments accompanied with the standard deviation represented as a vertical bar. The studied co-solutes in the phosphoramidation reactions were urea (closed square, ■), Tween 20 (closed triangle, ▲), Triton X-100 (open circle, ○), PEG 6000 (closed diamond, ◆), PEG 8000 (closed circle, ●), and glycerol (open square, □).

presence of these imidazole derivatives, however, indicated that only **2d** [4(5)-methylimidazole; Scheme 1] could substantially increase product yields for both DNA and RNA conjugation (Figure 2). The ability of compound **2d** as the only imidazole derivative to enhance product formation suggests that not only the nucleophilicity in the imidazole ring but also the steric hindrance imposed on the nucleophilic N in the imidazole moiety determine product yield in phosphoramidation reactions. Increasing nucleophilicity in the imidazole ring is a double-edged sword approach; it could stabilize the phosphoramidate bond in a phosphorimidazolide intermediate so effectively as to deter subsequent nucleophilic substitution required to attain desired products. We are currently synthesizing imidazole derivatives based on **2d** to further improve two-step phosphoramidation reaction yield.

Increase of Peptide Nucleophilicity to Promote POC Synthesis. We explored the relationship between peptide nucleophilicity and phosphoramidation yield. We previously demonstrated that diamino nucleophiles provided higher

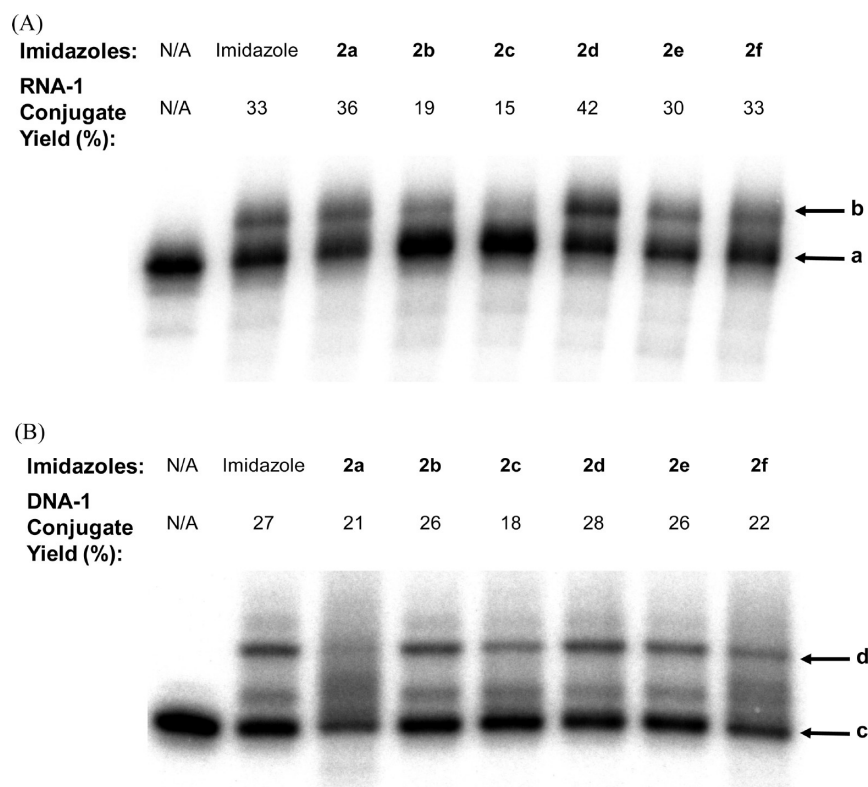


Figure 2. Influence of imidazole nucleophilicity on yields of two-step phosphoramidation reactions when conjugating **1** with (A) the ^{32}P -labeled TW17 RNA or (B) the ^{32}P -labeled single-stranded 3' primer DNA. Either imidazole or one of its derivatives (**2a–f**, Figure S1) was individually incorporated into a phosphoramidation reaction. The reaction product was purified by ethanol precipitation, analyzed by 8% urea-PAGE for the RNA-1 conjugate and 20% urea-PAGE for the DNA-1 conjugate, visualized and quantified by an Amersham Typhoon PhosphorImager. a, unreacted TW17 RNA; b, TW17 RNA-1 conjugate; c, unreacted 3' primer DNA; d, 3' primer DNA-1 conjugate.

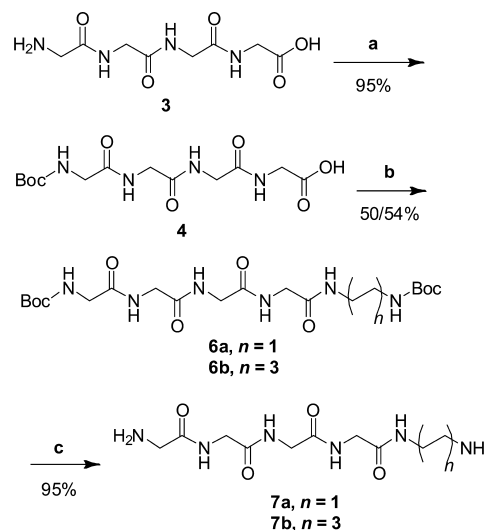
product yield in significantly shorter reaction time than monoamino nucleophile **1** in phosphoramidation reaction.²⁰

We thus reasoned that using modified peptides carrying additional amino groups would improve peptide nucleophilicity and further increase phosphoramidation reaction yields. Since we previously synthesized tetraglycine (**3**)²⁰ and it is also commercially available, we decided to use **3** as the starting material to yield two of its amino derivatives, the novel peptides **7a** and **7b**, each carrying an additional amino group appended on two or six carbon linkers (Scheme 2).

Synthesis of **7a** and **7b** started with Boc protection of **3** to give **4**. The Boc-protected **4** was initially acylated with **5a/5b** following our previous method for similar reactions in synthesis of **3** (EDC and Et_3N in DMF). Unexpectedly, the desired **6a/6b** was not produced after the reactions and their formations were not improved when DMAP was included in the reactions. We eventually adopted standard peptide coupling conditions²⁶ using EDC, HOBt, and DIPEA as reagents for the reactions and successfully synthesized **6a** and **6b**. Boc deprotection of **6a** and **6b** (TFA in DCM) and subsequent TFA removal by Amberlyst A-21²⁰ finally led to effective synthesis of the required **7a** and **7b**.

The successful synthesis of **7a** and **7b** allowed study of the two-step phosphoramidation reaction using **7a** and **7b** as the nucleophiles in the optimized reaction conditions. As expected, **7a** and **7b** were better nucleophiles than **1** and **3** when coupled with either the 3' primer DNA or the TW17 RNA to give higher reaction yield (Figure 3). Increasing the extent of amino functionality in the nucleophiles could contribute to higher yields in two-step phosphoramidation reactions. The results

Scheme 2. Synthesis of the Tetraglycine Derivatives **7^a**



^aReaction conditions: a, Di-*t*-Boc, NaOH/ H_2O /dioxane; b, (1) EDC, HOBt, (2) **5a/5b**, DIPEA, DMF; c, (1) TFA, DCM, (2) Amberlyst A-21, MeOH/DCM.

encouraged us to exploit the optimized two-step phosphoramidation reaction to synthesize POCs other than nucleic acid-3 conjugates because typical peptides usually have more amino groups than **7a** and **7b**. However, before employing the optimized two-step phosphoramidation reactions for synthesis

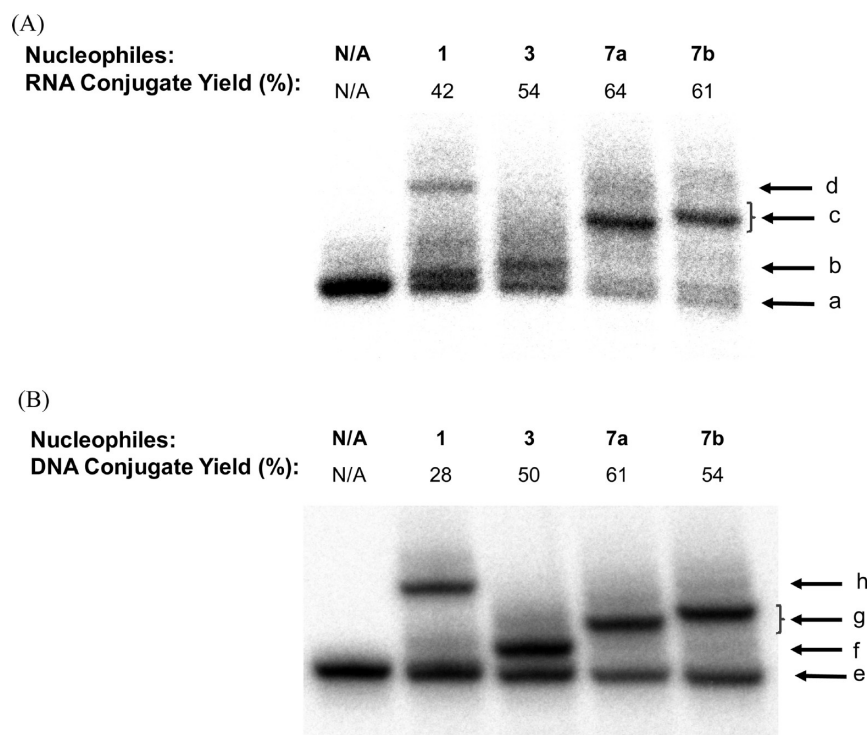


Figure 3. Phosphoramidation yield influenced by the nucleophilicity of nucleophiles when reacting with (A) the ^{32}P -labeled 17-mer TW17_{1–17} RNA and (B) the ^{32}P -labeled single-stranded 3' primer DNA. Each nucleophile (1, 3, 7a, or 7b) was conjugated with the nucleic acids according to the two-step phosphoramidation reactions optimized in this study. The reaction products were purified by ethanol precipitation, analyzed by 20% urea-PAGE, visualized and quantified by an Amersham Typhoon PhosphorImager. a, unreacted TW17_{1–17} RNA; b, TW17_{1–17} RNA-3 conjugate; c, TW17_{1–17} RNA-7a (or 7b) conjugate; d, TW17_{1–17} RNA-1 conjugate; e, unreacted 3' primer DNA; f, 3' primer DNA-3 conjugate; g, 3' primer DNA-7a (or 7b) conjugate; h, 3' primer DNA-1 conjugate.

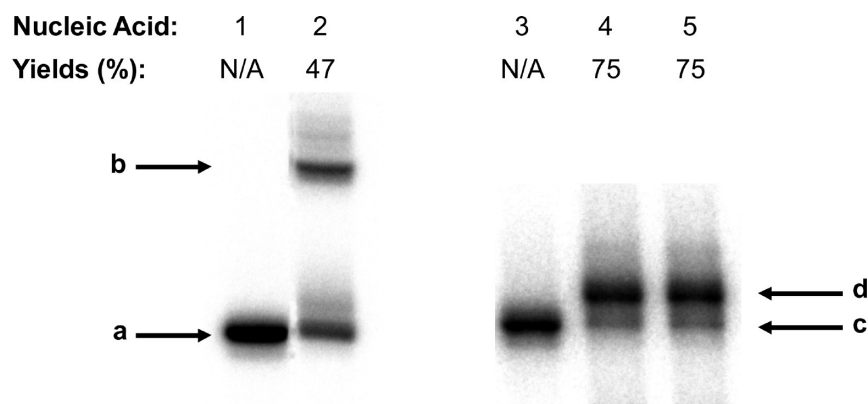


Figure 4. Autoradiogram of nucleic acids 1 (3' primer DNA), 2 (two-step phosphoramidation reaction between the 3' primer DNA and the Tat_{48–57} peptide), 3 (TW17 RNA), 4 (two-step phosphoramidation reaction between the TW17 RNA and 200 mM of the Tat_{48–57} peptide), and 5 (two-step phosphoramidation reaction between the TW17 RNA and 20 mM of the Tat_{48–57} peptide) analyzed by 8% urea-PAGE for the TW17 RNA samples and 20% urea-PAGE for the 3' primer DNA samples, visualized and quantified by an Amersham Typhoon PhosphorImager. The arrows indicate migrations of a, 3' primer DNA; b, 3' primer DNA–Tat_{48–57} peptide conjugate; c, TW17 RNA; d, TW17 RNA–Tat_{48–57} peptide conjugate.

of bioactive POCs, we desired to further increase POC yields by carrying out the reactions for DNA at higher temperatures.

Effects of Higher Temperatures on DNA Phosphoramidation Reactions. We previously concluded that RNA phosphoramidation reactions at 41 °C is the optimal reaction temperature because it balances reaction yield and RNA degradation at higher temperatures.²⁰ DNA, on the other hand, is far more chemically stable than RNA. Therefore, we investigated whether we could substantially improve yields of two-step DNA phosphoramidation reactions when performed above 41 °C (Figure S2). Indeed, we observed a steady increase

of product yields when having two-step phosphoramidation reactions at temperatures higher than 45 °C. DNA in the two-step phosphoramidation reactions, however, suffered from significant degradation at reaction temperatures above 55 °C. We, therefore, determined that 55 °C was the optimal temperature for two-step DNA phosphoramidation reactions and was used subsequently.

POC Synthesis by the Optimized Two-Step Phosphoramidation Reactions Using the Zero Linker Approach. We first employed the developed two-step phosphoramidation reactions to directly conjugate nucleic acids with a well-studied

Table 1. Survey of Aqueous-Phase Two-Step Nucleic Acid Phosphoramidation Reactions for Identifying the Optimal Reaction Condition to Give the Best Reaction Yields and to Be Exploited for POC Synthesis^a

DNA ^b /RNA ^{c,d}	co-solute	imidazole and derivatives	nucleophile	temperature (°C)	yield (%)
RNA ^c	N/A	imidazole	1	41	25%
RNA ^c	urea, 15% (w/v)	imidazole	1	41	18%
RNA ^c	Tween 20, 15% (w/v)	imidazole	1	41	30%
RNA ^c	Triton X-100, 15% (w/v)	imidazole	1	41	33%
RNA ^c	PEG 6000, 15% (w/v)	imidazole	1	41	32%
RNA ^c	PEG 8000, 15% (w/v)	imidazole	1	41	31%
RNA ^c	glycerol, 15% (w/v)	imidazole	1	41	30%
DNA ^b	N/A	imidazole	1	41	27%
DNA ^b	N/A	2a	1	41	21%
DNA ^b	N/A	2b	1	41	26%
DNA ^b	N/A	2c	1	41	18%
DNA ^b	N/A	2d	1	41	28%
DNA ^b	N/A	2e	1	41	26%
DNA ^b	N/A	2f	1	41	22%
RNA ^c	Triton X-100, 15% (w/v)	2a	1	41	36%
RNA ^c	Triton X-100, 15% (w/v)	2b	1	41	19%
RNA ^c	Triton X-100, 15% (w/v)	2c	1	41	15%
RNA ^c	Triton X-100, 15% (w/v)	2d	1	41	42%
RNA ^c	Triton X-100, 15% (w/v)	2e	1	41	30%
RNA ^c	Triton X-100, 15% (w/v)	2f	1	41	33%
RNA ^c	Triton X-100, 15% (w/v)	2d	3	41	54%
RNA ^c	Triton X-100, 15% (w/v)	2d	7a	41	64%
RNA ^c	Triton X-100, 15% (w/v)	2d	7b	41	61%
DNA ^b	N/A	2d	3	41	50%
DNA ^b	N/A	2d	7a	41	61%
DNA ^b	N/A	2d	7b	41	54%
DNA ^b	N/A	2d	1	45	31%
DNA ^b	N/A	2d	1	50	33%
DNA ^b	N/A	2d	1	55	37%
DNA ^b	N/A	2d	1	60	37%
DNA ^b	N/A	2d	Tat ₄₈₋₅₇ peptide	55	47%
RNA ^c	Triton X-100, 15% (w/v)	2d	Tat ₄₈₋₅₇ peptide	41	75%
DNA ^b	N/A	2d	cystamine	55	72%
RNA ^c	Triton X-100, 15% (w/v)	2d	cystamine	41	60%
DNA ^b	N/A	2d	cystamine, C(KFF) ₃ K peptide ^e	55	59%
RNA ^d	Triton X-100, 15% (w/v)	2d	cystamine, the C(KFF) ₃ K peptide ^e	41	75%

^aIt is noted that only the most important results from the co-solute effect study have been provided. The yields for the optimized two-step phosphoramidation reactions and for POC synthesis are bolded. ^b3' primer DNA. ^cTW17 RNA. ^dTW17₁₋₁₇ RNA. ^eConjugated to the nucleic acids by Michael addition.

CPP, the Tat₄₈₋₅₇ peptide,^{12,18} in the presence of no linking molecules between them, the zero linker approach. The Tat₄₈₋₅₇ peptide was used to serve the purpose of a vector to traffic DNA into mammalian cells validated by subsequent biological analysis. The Tat₄₈₋₅₇ peptide has 9 nucleophilic amino groups (3 primary amino and 6 secondary amino groups) in each molecule. Since increasing numbers of nucleophilic functionalities in nucleophiles was likely to enhance POC yields (Figure 3), we reasoned that using the Tat₄₈₋₅₇ peptide as the nucleophile could decrease the molar ratios of nucleophiles to nucleic acids well below 585, the required ratio for **1** and **3** as the nucleophiles, while retaining similar reaction yields in the optimized two-step phosphoramidation reactions.

As expected, the optimized two-step phosphoramidation reactions by the zero linker approach only required 62.5 as ratio of Tat₄₈₋₅₇ peptide to nucleic acids to achieve a 47% yield for the 3' primer DNA–Tat₄₈₋₅₇ peptide conjugate and a 75% yield for the TW 17 RNA–Tat₄₈₋₅₇ peptide conjugate (Figure 4 and

Table 1). Figure 4 also clearly indicates that only a nucleic acid molecule was covalently linked to the Tat₄₈₋₅₇ peptide even though the Tat₄₈₋₅₇ peptide has 9 nucleophilic functionalities for phosphoramidation reactions. In addition, multiple nucleophilic functionalities in the Tat₄₈₋₅₇ peptide suggested that each amino group in the Tat₄₈₋₅₇ peptide has the potential to engage in a phosphoramidation reaction to contribute to the observed POC in Figure 4. Interestingly, the product complexity did not seem to be an issue, because we observed significantly lower POC yields in the same phosphoramidation reactions when replacing the Tat₄₈₋₅₇ peptide, which has glycine in the N-terminus, with the Tat₄₇₋₅₇ peptide, which has tyrosine in the N-terminus (Figure S3). Similar preference for glycine in the N terminus was also observed when an *E. coli* CPP, the (KFF)₃K peptide, and its derivatives were phosphoramidated with the 3' primer DNA (Figure S3). These results implicated the N-terminus amino group in a peptide as the primary nucleophile in phosphoramidation reactions and its reactivity strongly affected by steric hindrance

imposed by the side chain of the N-terminus amino acid residue. The N-terminus glycine in a peptide emerges as the best nucleophile in phosphoramidation reactions because very limited steric hindrance would be enacted by the hydrogen atom, the side chain of glycine. The preference of glycine over other amino acids in the N-terminus of peptides for phosphoramidation-prepared POC formation is also consistent with the properties of **2d** [4(5)-methylimidazole] to give the best phosphoramidation yield (Figure 2). Consequently, despite the presence of primary and secondary amino groups in typical peptides, the N-terminus amino group is clearly the best nucleophile to participate in nucleophilic substitution reactions with nucleic acid phosphorimidazolides. The N-terminus amino group of a peptide as the favorite nucleophile in nucleic acid phosphoramidation attains more specific reactions and produces relatively structurally uniform POC conjugates. Moreover, glycine in the N-terminus of peptides should be the choice for synthesis of phosphoramidation-prepared POCs because it has the least steric hindrance among amino acids.

We characterized the acquired POCs by MALDI-TOF MS to determine the molecular mass. We initially wondered whether the molecular mass of a phosphoramidation-prepared POC could be measured by more sensitive positive-mode MALDI-TOF MS. Adopting positive-mode MALDI-TOF MS required the use of acidic MALDI-TOF matrices, reported to be detrimental to phosphoramidate bonds in DNA during analysis and lead to DNA degradation.²⁷ Therefore, we performed a control experiment prior to positive-mode MALDI-TOF MS analysis by incubating the gel-purified 3' primer DNA-Tat₄₈₋₅₇ peptide conjugate in an acidic MALDI-TOF matrix solution composed of 2,3,4-trihydroxyacetophenone, 2,4,6-trihydroxyacetophenone, and ammonium citrate for 3 h. We were pleased to observe that the phosphoramidate bond linking the 3' primer DNA and the Tat₄₈₋₅₇ peptide was significantly inert in the MALDI-TOF matrix solution because only 5% of the phosphoramidation-prepared POC were hydrolyzed at the end of incubation (Figure S4).

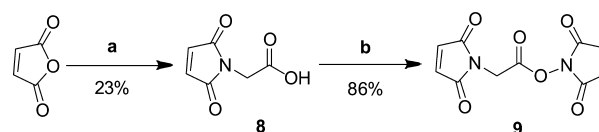
The molecular mass of the 3' DNA primer-Tat₄₈₋₅₇ peptide conjugate was ultimately confirmed by MALDI-TOF MS ($[M+H]^+ = 7416.096$; Table 1 and Supporting Information). We, however, were not able to determine the molecular mass of the TW17 RNA-Tat₄₈₋₅₇ peptide conjugate because the TW17 RNA was synthesized by in vitro transcription of T7 RNA polymerase to render a heterogeneous molecular mass of the RNA.²⁸ In addition, the size of the TW17 RNA-Tat₄₈₋₅₇ peptide conjugate (~30 kD) prevents an accurate measurement of the molecular mass by MALDI-TOF MS.

Optimizing the Two-Step Phosphoramidation Reactions for Synthesis of POCs Containing the Cystamine-9 Linker. We synthesized POCs by using cystamine in two-step phosphoramidation reactions in order to introduce a cystamine-9 linker in nucleic acids for subsequent peptide coupling reactions. The cystamine-9 linker was harnessed for two purposes: (1) the disulfide linkage in cystamine potentially reduced in vivo to release oligonucleotides from POCs which could be essential for oligonucleotides to more specifically silence target genes in biological systems, and (2) the maleimide group in **9** to perform the more effective Michael addition reaction which would lower ratios of peptides to nucleic acids in POC synthesis. Reducing ratios of peptide to nucleic acids in synthesis of phosphoramidation-prepared POCs has important economic significance, as fewer peptides

will be wasted during POC synthesis. We were thus motivated to pursue the cystamine-9 linker strategy for more effective POC synthesis.

To achieve synthesis of the cystamine-9 linker-included POCs, we decided to synthesize **9**, a *N*-maleoyl amino acid succinimidyl ester. In addition, we desired to develop a method for general synthesis of *N*-maleoyl amino acid succinimidyl esters for POC synthesis in the future. We succeeded in synthesizing **9** (Scheme 3) by adopting a reported procedure to

Scheme 3. Synthesis of the *N*-Maleoyl Amino Acid Succinimidyl Ester **9**^a

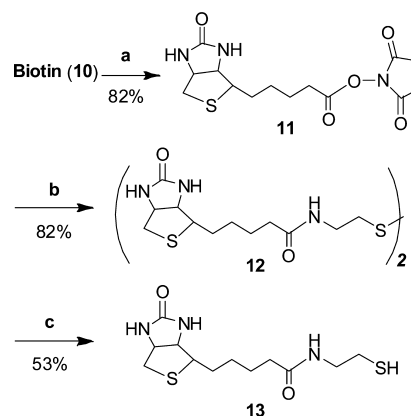


^aReaction conditions: a, (1) glycine, glacial AcOH, 16 h (2) reflux, 8 h; b, NHS, DCC, THF, 16 h.

acquire **8**²² and following up a NHS ester formation reaction to give the desired **9** with good yield. We are improving the method for synthesis of **9** and developing a more universal approach to synthesize other useful *N*-maleoyl amino acid succinimidyl esters.

When applying **9** for POC synthesis, we soon realized the importance of optimizing the conjugation reactions involving both functionalities in **9**, i.e., acylation and Michael addition reactions to relieve the cost burden when purchasing peptides from commercial vendors. Therefore, we synthesized **11** and **13** (Scheme 4) as model compounds to optimize the reactions of **9**

Scheme 4. Synthesis of **13**, a Thiol Derivative of Biotin^a



^aReaction conditions: a, NHS, DCC, pyridine, DMF, 24 h; b, cystamine, Et₃N, DMF/H₂O, 16 h; c, DTT, Et₃N, DMF, 3 h.

for more effective conjugation of nucleic acids with peptides. The reasons for using **11** and **13** to determine optimal reaction conditions of **9** for POC synthesis were that these compounds have appropriate functionalities to engage in one of the conjugation reactions. In addition, both compounds have biotin tags to separate reaction products from reactants by SA_v gel shift assay²³ in case of an inability to separate nucleic acid samples by urea-PAGE. Synthesis of **11** was reported by us previously.²⁰ Starting from **11**, a facile acylation reaction successfully produced **12** (82%), which was subsequently reduced in the presence of DTT to give the desired **13** (53%).

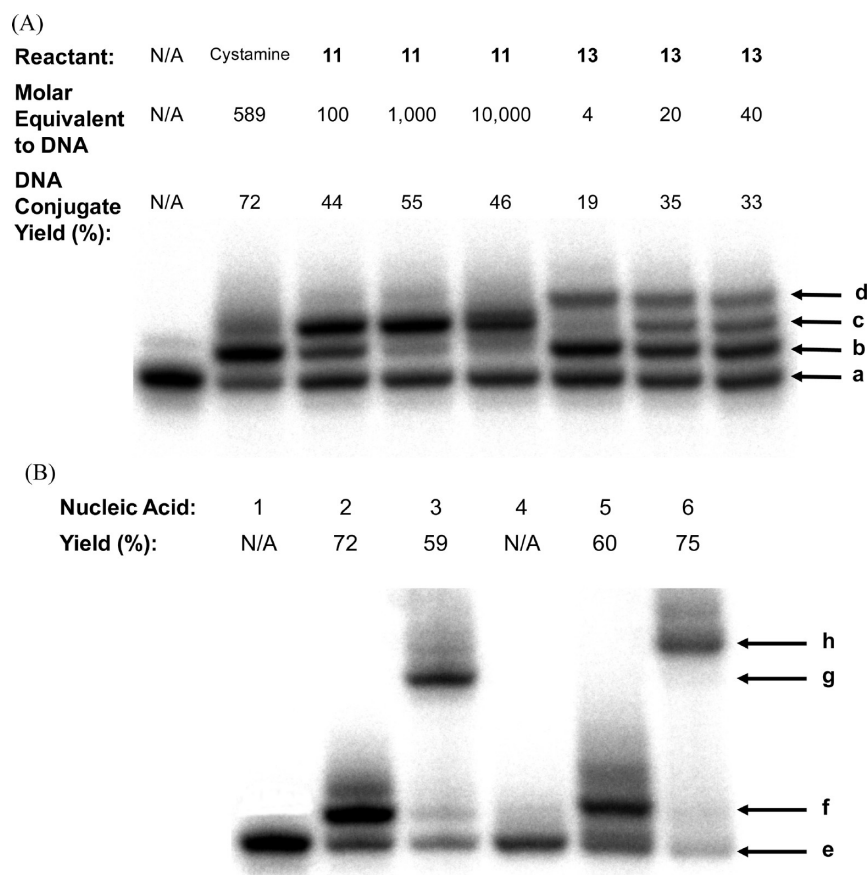


Figure 5. Optimization of the reactions involving AMAS (**9**) and synthesis of POCs in the presence of the cystamine-**9** linker. (A) The reactions of **9** were optimized by using **11** and **13**. The ^{32}P -labeled single-stranded 3' primer DNA (**a**) was first coupled with cystamine to acquire the DNA-cystamine conjugate (Chart S1; Supporting Information) (**b**). The DNA-cystamine conjugate was subsequently reacted with various molar equivalents of **11** to determine the appropriate molar equivalent able to give the best yield of the DNA-cystamine-**11** conjugate (Chart S1; Supporting Information) (**c**). A molar equivalent of 1000 was adopted to react the DNA-cystamine conjugate with **9** to yield the DNA-cystamine-**9** conjugate (Chart S1; Supporting Information) (**c**), which was later coupled with various molar equivalents of **13**. It was determined that the molar equivalent of 20 was sufficient to have the best yield of the DNA-cystamine-**9**-**13** conjugate (Chart S1; Supporting Information) (**d**). Each reaction product was purified by ethanol precipitation, analyzed by 20% urea-PAGE, visualized, and quantified by an Amersham Typhoon PhosphorImager. **a**, the unreacted 3' primer DNA; **b**, the 3' primer DNA-cystamine conjugate; **c**, the 3' primer DNA-cystamine-**11** (or -**9**) conjugate; **d**, the 3' primer DNA-**9**-**13** conjugate. (B) The cystamine-**9** linker-prepared POCs were synthesized by the optimized reaction conditions developed in Figure 5A. The nucleic acids in the autoradiogram contains **1** (the 3' primer DNA), **2** (the cystamine-modified 3' primer DNA preparation reaction), **3** (the 3' primer DNA-C(KFF) $_3$ K peptide conjugate preparation reaction), **4** (the 17-mer TW17 $_{1-17}$ RNA), **5** (the cystamine-modified TW17 $_{1-17}$ RNA preparation reaction), and **6** (the TW17 $_{1-17}$ RNA-C(KFF) $_3$ K peptide conjugate preparation reaction). The arrows indicate migrations of **e**, the 3' primer DNA or TW17 $_{1-17}$ RNA; **f**, the cystamine-modified oligonucleotides; **g**, the 3' primer DNA-C(KFF) $_3$ K peptide conjugate; **h**, the TW17 $_{1-17}$ RNA-C(KFF) $_3$ K peptide conjugate.

We first used **11** to optimize the acylation reaction between the cystamine-modified 3' primer DNA and **9**. The 3' primer DNA was initially conjugated with cystamine according to the optimized two-step phosphoramidation reaction reported in this study with a yield of 72% (Figure 5A and Table 1). When reacting the cystamine-modified 3' primer DNA with **11**, we were delighted to observe that the ^{32}P -labeled 3' primer DNA and its structure-modified derivatives were well separated in urea-PAGE so that the potentially ambiguous SAv gel shift assay was not required. Moreover, the results from the reactions of cystamine-modified 3' primer DNA with various concentrations of **11** clearly indicated that a value of 1000 for the molar ratio of **11** to the 3' primer DNA gave the best yield for the acylation reaction and was adopted for the similar reaction between the cystamine-modified 3' primer DNA and **9**. The acquired **9**-cystamine-modified 3' primer DNA was employed to react with a series of **13** concentrations and to identify the

appropriate molar ratio of **13** to nucleic acids for attaining the best yield in the Michael addition reaction (Figure 5A). A value of 20 for the molar ratio of **13** to the **9**-cystamine-modified 3' primer DNA was sufficient to provide the best yield for the studied Michael addition reaction and was determined to be the optimal condition for POC synthesis.

The optimized reactions for **9** were successfully applied to conjugating nucleic acids with the C(KFF) $_3$ K peptide, the derivative of a previously reported synthetic CPP (KFF) $_3$ K peptide,¹⁷ to obtain the corresponding POCs with excellent yields (59–75%; Figure 5B and Table 1). It is noted that we used a shorter version of TW17 RNA, TW17 $_{1-17}$ RNA, in order to measure the molecular mass of the desired RNA POC, TW17 $_{1-17}$ RNA-C(KFF) $_3$ K peptide conjugate, subsequently by MALDI-TOF MS. As expected, the identity of each synthesized POCs was successfully characterized by MALDI-TOF MS to determine the molecular mass (Table 1 and

Supporting Information). The two-step phosphoramidation reactions for POC synthesis in the presence of the cystamine-9 linker demonstrated advantages over POC synthesis by the phosphoramidation reactions performed with the zero linker approach. The incorporation of the cystamine-9 linker in POC synthesis offers both higher reaction yields (Figures 4 and 5B) and a lower demand for peptides in POC synthesis (20 as the molar ratio of peptide to oligonucleotide in this reaction) than the zero linker strategy for POC synthesis. We expect that the use of linkers similar to the cystamine-9 bridge will have more leverage for future POC synthesis.

Cytotoxicity of Phosphoramidation-Prepared POCs to a Human Cell Line. We understood that the phosphoramidate linkage has to exhibit low to no toxicity to human beings before phosphoramidation-prepared POCs would be administrated in clinical applications. Therefore, we exploited the two-step phosphoramidation reactions using the zero linker approach to synthesize more of the POC, the 3' primer DNA-Tat₄₈₋₅₇ peptide conjugate (Figure 4), and to study toxicity of the POC to human A549 cells. We chose the zero linker approach rather than using the cystamine-9 linker strategy to synthesize POC for the toxicity study because we want to focus only on the toxic effects of the introduced phosphoramidate bond in the 3' primer DNA-Tat₄₈₋₅₇ peptide conjugate. We were satisfied to find that the inoculated 3' primer DNA-Tat₄₈₋₅₇ peptide conjugate with concentrations up to 10 μM showed no toxicity to human A549 cells after 24 h inoculation (Figure 6).

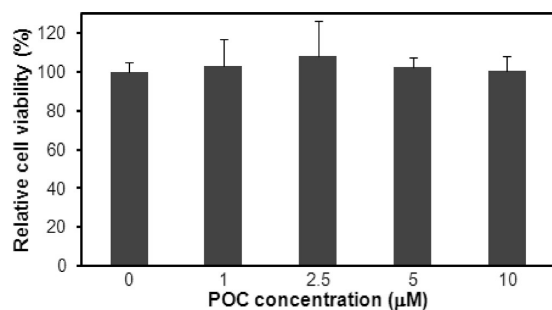


Figure 6. Undetectable cytotoxicity of phosphoramidation-prepared POCs to human A549 cells after 24 h inoculation. Human A549 cells were incubated with increased concentrations of the phosphoramidation-prepared POC, the 3' primer DNA-Tat₄₈₋₅₇ peptide conjugate (0–10 μM). After 24 h inoculation, cell viability for each sample containing a specified POC concentration was determined by the MTT assay.

Therefore, there is no detectable toxicity of phosphoramidate linkages in POCs to human cells in these studied concentrations after 24 h inoculation, and we validated the potentially safe use of phosphoramidation-prepared POC as therapeutic agents for treating human diseases.

Uptake of Phosphoramidation-Prepared POCs by a Human Cell Line. We had already shown that phosphoramidate bonds in POCs had no toxicity to human A549 cells after 24 h inoculation (Figure 6). The potential evidence of human safety of phosphoramidate linkages in POCs encouraged us to carry out additional studies to explicate effects of phosphoramidate bonds on the cellular permeability ability of CPPs in phosphoramidation-prepared POCs. We again used the 3' primer DNA-Tat₄₈₋₅₇ peptide conjugate as the model POC to study the uptake of POCs by human A549 cells. To unambiguously demonstrate uptake of the 3' primer

DNA by human A549 cells, we labeled the 3' primer DNA with the fluorophore FITC by a depurination method²⁵ before the DNA was conjugated with the Tat₄₈₋₅₇ peptide by the two-step phosphoramidation reaction developed in this study. Acquisition of the FITC-labeled 3' primer DNA-Tat₄₈₋₅₇ peptide conjugate allowed us to study permeability of the POC into human A549 cells by flow cytometry, fluorescent microscopy, and confocal laser scanning microscopy.

The results from flow cytometry analysis clearly showed that the FITC-labeled 3' primer DNA-Tat₄₈₋₅₇ peptide conjugate was significantly taken up by human A549 cells after 24 h inoculation of the POC (Figure 7). In addition, the association of the FITC-labeled 3' primer DNA-Tat₄₈₋₅₇ peptide conjugate with A549 cells was revealed by fluorescent microscopy studies which indicated colocalization of fluorescence signals with intact A549 cells (Figure S5). Finally, we performed confocal laser scanning microscopy to determine whether the observed fluorescence signals were contributed by the FITC-labeled 3' primer DNA-Tat₄₈₋₅₇ peptide conjugate trafficked inside A549 cells or by the FITC-labeled POC adsorbed on the cell membrane. Consistent with our expectation, the results from the confocal laser scanning microscopy study unequivocally demonstrated that the FITC-labeled 3' primer DNA-Tat₄₈₋₅₇ peptide conjugate was taken up by A549 cells rather than merely adsorbed on the cell membrane after 24 h inoculation (Figure 7). The results of these biological uptake studies support the premise that a phosphoramidate bond does not alter cellular permeability activity of CPPs in phosphoramidation-prepared POCs and would not have a negative impact on cellular delivery and targeting of phosphoramidation-prepared POCs when administrated as therapeutic agents in the clinic.

DISCUSSION

We have significantly improved reaction yields of two-step nucleic acid phosphoramidation by studying the contribution of three crucial factors, co-solute effect, imidazole nucleophilicity and structure, and the advantage of multiple nucleophilic functionalities in nucleophiles (Figures 1–3, Scheme 1, and Table 1). Moreover, we successfully employed the zero linker strategy of the optimized two-step phosphoramidation reactions to effectively conjugate a well-studied CPP TAT₄₈₋₅₇ peptide with DNA or RNA with corresponding POC yields of 47–75% (Figure 4, Table 1, and Scheme 5). We also developed a more effective phosphoramidation method for DNA/RNA POC synthesis by exploiting a cystamine-9 linker to acquire corresponding POC yields of 59–75% (Figure 5, Table 1, and Scheme 5). The phosphoramidation-synthesized DNA POC, 3' primer DNA-Tat₄₈₋₅₇ peptide conjugate, showed no cytotoxicity to human A549 cells at POC concentrations up to 10 μM after 24 h inoculation and established the potentially safe use of phosphoramidation-synthesized POCs in clinical applications (Figure 6). In addition, the FITC-labeled 3' primer DNA-Tat₄₈₋₅₇ peptide conjugate was successfully trafficked into the human A549 cell line as demonstrated by studies of flow cytometry, fluorescent microscopy, and confocal laser scanning microscopy (Figures 7 and S5). These results provide evidence that the presence of phosphoramidate bonds in CPP-containing POCs will not impair the cell permeability of CPPs in POCs and suggests the potential development of target-delivered therapeutic reagents based on nucleic acid phosphoramidation reactions. The current study corroborates the assertion that the advanced

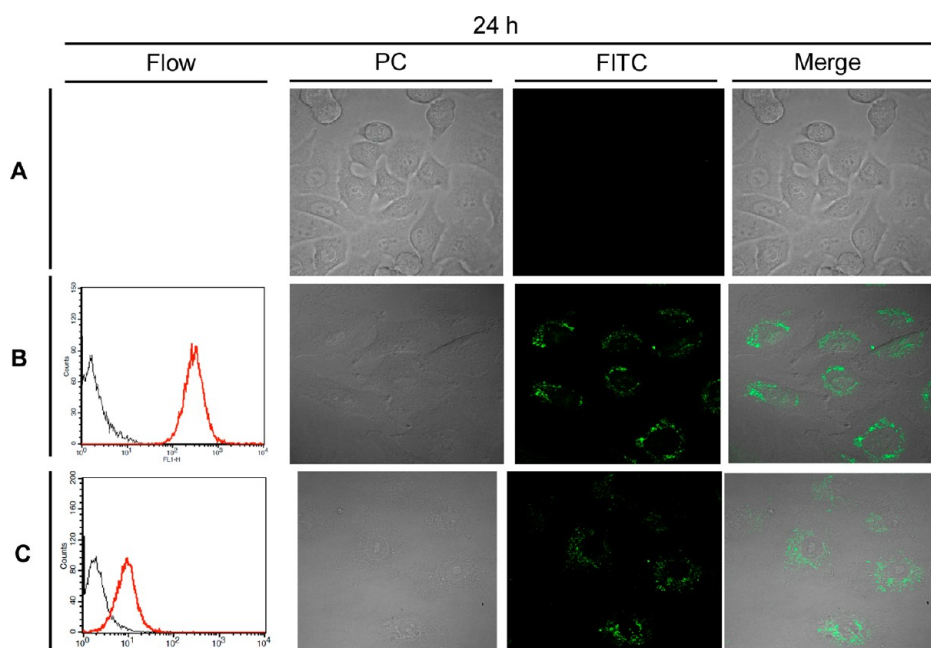
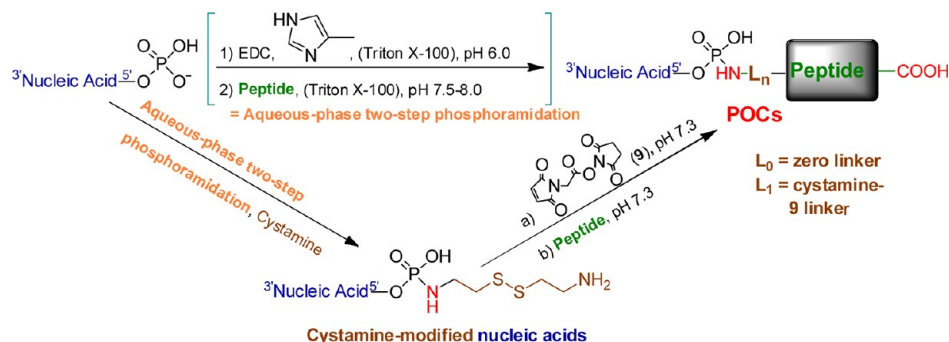


Figure 7. Uptake of phosphoramidation-prepared POCs by human A549 cells. Human A549 cells were inoculated with $5 \mu\text{M}$ of the FITC-labeled Tat_{48-57} peptide or the phosphoramidation-prepared POC, the FITC-labeled 3' primer DNA- Tat_{48-57} peptide conjugate, for 24 h and followed by analysis with flow cytometry and confocal laser scanning microscopy. For flow cytometry, cells were washed and harvested with trypsin/EDTA before analysis. A549 cells for the confocal laser scanning microscopy study were washed three times with PBS and analyzed immediately. The studied A549 cell samples included: **A**, cells not treated with either the Tat_{48-57} peptide or the 3' primer DNA- Tat_{48-57} peptide conjugate; **B**, cells incubated with the FITC-labeled Tat_{48-57} peptide for 24 h; **C**, cells incubated with the FITC-labeled 3' primer DNA- Tat_{48-57} peptide conjugate for 24 h. PC, phase contrast.

Scheme 5. Optimized Aqueous-Phase Two-Step Phosphoramidation Reactions for POC Synthesis



aqueous-phase two-step phosphoramidation reactions are an efficient and effective approach to synthesize bioactive POCs.

The use of urea and other co-solutes in phosphoramidation reactions deserves additional discussion to explicate their roles. The current study clearly demonstrates that urea could not carry out its expected function of denaturing nucleic acids to confer higher product yields for phosphoramidation reactions. Instead, urea caused reduction of reaction yield because of direct participation of urea in nucleophilic substitution preventing the desired product formation (Figure 1).²⁰ We had reached a similar conclusion on DNA phosphoramidation reactions but had observed the beneficial presence of urea in RNA phosphoramidation reactions previously.²⁰ The discrepancy of the effect of urea in RNA phosphoramidation reactions is attributed to the shortcomings of the SAV gel shift assay used in the previous study. A standard SAV gel shift assay relies on strong interaction between biotin and SAV to separate biotin-tagged from non-biotin-tagged biomacromolecules. Unfortunately, in previously studied nucleic acid phosphoramidation

reactions, SAV-retarded nucleic acids co-migrated with polymerized nucleic acids, byproducts of the phosphoramidation reactions,²⁹ and were indistinguishable in the standard SAV gel shift assay. The co-migration resulted in an overestimation of the desired RNA reaction products (Ko and Wang, unpublished results). We had carefully optimized the concentrations and ratios of EDC to nucleic acids to significantly suppress the unwanted polymerization of nucleic acids (less than 5%) in not only the two-step phosphoramidation reactions reported in this study, but also the one-step phosphoramidation versions (Wang et al., manuscript in preparation). The more accurate determination of the phosphoramidation reaction yield was attained by analysis of urea-PAGE, which depends solely on the size and the charge of nucleic acids to achieve separation and unambiguously resolved the molecular difference of reactants and phosphoramidation products, resulting in more faithful calculations of product formation. Therefore, urea-PAGE was a major analytical method employed in the current study. Consequently, inclusion of urea as co-solute in any nucleic

acid phosphoramidation reactions should be avoided, as urea has a negative impact on the reactions by reducing the yield of the desired product. On the contrary, more inert and hydroxyl group-based co-solutes such as Triton X-100 will perform the anticipated function of RNA denaturation and deliver higher product yield in phosphoramidation reactions (Figure 1A).

In addition to the effects of co-solutes in phosphoramidation reactions, the chemoselectivity of nucleic acids toward specific primary amino groups of peptides in the zero linker approach of the phosphoramidation reactions is significant (Figure S3). Specifically, we observed that nucleic acids in zero-linker two-step phosphoramidation reactions primarily reacted with the α -amino group in N-terminus glycine residue of a peptide and only one nucleic acid was conjugated to each peptide molecule. This phenomenon came as a pleasant surprise, as we were initially concerned about the multiple nucleophilic functionalities in a typical peptide and their potential to engage in phosphoramidation reactions. We anticipated that it would be unlikely to have specific phosphoramidation reactions for controllable POC synthesis and expected undesirable complicated structures of POC products which might impede the use of phosphoramidation reactions for synthesis of POCs as therapeutic agents or scientific tools. Therefore, it was very exciting to find that the phosphorimidazolide intermediates of nucleic acids had chemoselectivity and preferred to react with the N-terminal α -amino group and with glycine in the N-terminus of a peptide.

The chemoselective property of the phosphoramidation reactions between nucleic acids and peptides is intriguing because the basicity of the primary amino group in the side chain of lysine ($pK_a = 10.54$),³⁰ which is one of the major components in the peptides in this study, is higher than that of the α -amino group in glycine ($pK_a = 9.78$).³⁰ When considering the basicity and nucleophilicity of the primary amino groups in glycine and lysine, we would predict that the phosphorimidazolide intermediates of nucleic acids are more likely to react with the ϵ -amino group of lysine than with the α -amino group of glycine in these peptides. In addition, multiple primary amino groups in the peptides would also implicate that conjugations of nucleic acids with a peptide by zero-linker two-step phosphoramidation reactions should produce complicated structural variations of POC products because of the likelihood of multiple nucleic acid conjugations with each peptide.

Fortunately, the ϵ -amino groups of lysine in the peptides did not demonstrate appreciably reactivity with the phosphorimidazolide intermediates of nucleic acids, and each peptide was only conjugated with one molecule of nucleic acid (Figure 4). We speculate that the ϵ -amino groups of lysine in the peptides might have been buried in the interior of three-dimensional peptide structures and were unavailable for phosphoramidation reactions. NMR analysis and computational studies of these peptide structures in water are required to provide essential information on the steric environments of these primary amino groups in the peptides and their relationship to the chemoselectivity of nucleic acid phosphoramidation reactions.

The achievement of only one nucleic acid unit conjugated with each peptide molecule in zero-linker two-step phosphoramidation reactions provided relatively uniform and predictable POC structures and could be explained by a strong electrostatic attraction between nucleic acids and peptides. Nucleic acids are well-known polyelectrolytes laden with negatively charged phosphate groups at a physiological pH. On the other hand,

the CPPs studied here all have ample lysine or lysine and arginine residues in their structures to contribute high positive charge density in the peptides at neutral pH. Consequently, when the α -amino group in the N-terminal glycine of a CPP underwent a phosphoramidation reaction with a nucleic acid, the phosphoramidate bond brought these oppositely charged components in close proximity to enact strong electrostatic forces between the CPP and the nucleic acid. Extensive electrostatic forces from CPP–nucleic acid interactions would immediately shield other primary amino groups in the CPP from having further phosphoramidation reactions and attain a single nucleic acid conjugation in each CPP. In fact, the electrostatic attractive forces between nucleic acids and CPPs were so strong that even boiling the nucleic acid–CPP complexes for minutes in the presence of 8 M urea did not completely remove CPPs from nucleic acids as revealed by standard urea-PAGE (Su and Wang, unpublished results). Moreover, the sizes of nucleic acids (6037 amu for the 3' primer DNA, 5440 amu for the TW17_{1–17} RNA, and ~28 000 amu for the TW17 RNA) are far larger than those of CPPs (1396 amu for the Tat_{48–57} peptide and 1517 amu for the C(KFF)₃K peptide) so that a nucleic acid molecule could adsorb and exclude each CPP from contacting a second nucleic acid. Similarly, strong electrostatic attraction between the Tat_{48–57} peptide and nucleic acids could play a prominent role to enhance POC formation observed in Figure 4.

Using a nucleic acid–CPP bridge similar to the cystamine-9 linker further alleviates the potential complexity problem of POC products synthesized by phosphoramidation reactions. The use of molecular bridges such as the cystamine-9 linker for POCs synthesized by phosphoramidation reactions took advantage of a more defined conjugation reaction between nucleic acids and CPPs, which was achieved by the more specific Michael addition reaction between the thiol group in CPPs and the maleimide moiety in phosphoramidation-modified nucleic acids. Maleimides have specific reactivity for thiol groups in the pH range 6.5–7.5.³¹ The other benefit of introducing molecular bridges analogous to the cystamine-9 linker is a significantly reduced requirement for the amount of CPP for effective POC synthesis (Figure 5B), which again could be attributed to effectiveness of the Michael addition reaction. The outstanding properties of Michael addition to convey more effective and chemospecific reactions and to deliver more structure-defined POC products justify the preferred choice of adopting the maleimide-containing bridges for POCs synthesized by aqueous-phase two-step phosphoramidation reactions.

In summary, this study significantly improved the aqueous-phase two-step phosphoramidation reactions and demonstrated the potential of either zero linker or linkers containing maleimide moieties of phosphoramidation reactions for effective and efficient POC synthesis. In addition, chemoselectivity of the advanced two-step nucleic acid phosphoramidation reactions supports the synthesis of POCs with expected structures, which is essential to evaluating POC functions in clinical applications. Furthermore, the versatility of phosphoramidation reactions enables us to append diverse functional groups to nucleic acids for subsequent reactions and further facilitate POC synthesis. Finally, the advanced nucleic acid phosphoramidation reaction is not restricted to POC synthesis for acquiring nucleic acid-based therapeutic agents useful in clinic. It can be exploited to conjugate nucleic acids with various tag molecules invaluable in research. For example,

we had developed a facile and low-cost universal fluorescent labeling method for DNA and RNA based on the advanced two-step phosphoramidation reaction (Wang et al., manuscript in preparation). We expect broader applications of nucleic acid phosphoramidation reactions in research and in clinic in the future.

■ ASSOCIATED CONTENT

Supporting Information

Full details of supporting figures, scheme and chart referenced in the text, NMR and MS spectra for new compounds (**4**, **6a**, **6b**, **7a**, **7b**, **9**, **12**, and **13**) and MALDI-TOF spectra for three POCs. This material is available free of charge via the Internet at <http://pubs.acs.org>.

■ AUTHOR INFORMATION

Corresponding Author

*Department of Medicinal and Applied Chemistry, Kaohsiung Medical University, Kaohsiung, 80708, Taiwan; E-mail: tzupinw@cc.kmu.edu.tw; Tel: +886-07-312-1101, ext. 2756; Fax: +886-07-312-5339 (T.-P. Wang). School of Medicine, Graduate Institute of Medicine, College of Medicine, Kaohsiung Medical University, Kaohsiung, 80708, Taiwan; Division of Infectious Diseases, Department of Internal Medicine, Kaohsiung Medical University Hospital, Kaohsiung Medical University, Kaohsiung, 80708, Taiwan; E-mail: infchen@gmail.com (Y.-H. Chen).

Notes

The authors declare no competing financial interest.

■ ACKNOWLEDGMENTS

We thank Dr. Susan Fetzter for critical reading of the manuscript. We also thank Drs. Shih-Shin Liang and Chi-Yu Lu for providing expertise in MALDI-TOF MS analysis. This work was supported with grants from the National Science Council of Taiwan awarded to T.-P. W. (99-2113-M-037-008 and 100-2113-M-037-008-). M. H. W. is supported by the undergraduate research program funded by National Science Council of Taiwan (101CFD2100044).

■ ABBREVIATIONS

POCs, peptide–oligonucleotide conjugates; Tat_{48–57} peptide, amino acid residues 48 to 57 of the HIV Tat protein; siRNA, small interference RNA; miRNA, microRNA; CPPs, cell-penetrating peptides; CTPs, cell-targeting peptides; urea-PAGE, urea polyacrylamide gel electrophoresis; SA_v, streptavidin; HOBt, 1-hydroxybenzotriazole; DIPEA, *N,N*-diisopropylethylamine; EDC, 1-ethyl-3-(3-dimethylaminopropyl)-carbodiimide; TFA, trifluoroacetic acid; AMAS, *N*-(α -maleimidoacetoxy) succinimide ester; NHS, *N*-hydroxysuccinimide; DCC, *N,N'*-dicyclohexylcarbodiimide; Et₃N, triethylamine; DTT, DL-dithiothreitol; EPPS, 3-[4-(2-hydroxyethyl)-1-piperazinyl]propanesulfonic acid; DEPC, diethylpyrocarbonate; MTT, methylthiazole tetrazolium; FITC, fluorescein isothiocyanate; PBS, phosphate buffer saline; DMAP, 4-dimethylaminopyridine.

■ REFERENCES

- (1) Bennett, C. F., and Swayze, E. E. (2010) RNA targeting therapeutics: molecular mechanisms of antisense oligonucleotides as a therapeutic platform. *Annu. Rev. Pharmacol. Toxicol.* **50**, 259–293.
- (2) Douglas, S. M., Bachelet, I., and Church, G. M. (2012) A logic-gated nanorobot for targeted transport of molecular payloads. *Science* **335**, 831–834.
- (3) Juliano, R., Bauman, J., Kang, H., and Ming, X. (2009) Biological barriers to therapy with antisense and siRNA oligonucleotides. *Mol. Pharmaceutics* **6**, 686–695.
- (4) Whitehead, K. A., Langer, R., and Anderson, D. G. (2009) Knocking down barriers: advances in siRNA delivery. *Nat. Rev. Drug Discovery* **8**, 129–138.
- (5) Watts, J. K., and Corey, D. R. (2012) Silencing disease genes in the laboratory and the clinic. *J. Pathol.* **226**, 365–379.
- (6) Burnett, J. C., and Rossi, J. J. (2012) RNA-based therapeutics: current progress and future prospects. *Chem. Biol.* **19**, 60–71.
- (7) Juliano, R. L., Ming, X., and Nakagawa, O. (2012) The chemistry and biology of oligonucleotide conjugates. *Acc. Chem. Res.* **45**, 1067–1076.
- (8) Ivanova, G. D., Arzumanov, A., Abes, R., Yin, H., Wood, M. J. A., Lebleu, B., and Gait, M. J. (2008) Improved cell-penetrating peptide-PNA conjugates for splicing redirection in HeLa cells and exon skipping in mdx mouse muscle. *Nucleic Acids Res.* **36**, 6418–6428.
- (9) Ming, X., Alam, M. R., Fisher, M., Yan, Y., Chen, X., and Juliano, R. L. (2010) Intracellular delivery of an antisense oligonucleotide via endocytosis of a G protein-coupled receptor. *Nucleic Acids Res.* **38**, 6567–6576.
- (10) Nakagawa, O., Ming, X., Huang, L., and Juliano, R. L. (2010) Targeted intracellular delivery of antisense oligonucleotides via conjugation with small-molecule ligands. *J. Am. Chem. Soc.* **132**, 8848–8849.
- (11) Said Hassane, F., Saleh, A., Abes, R., Gait, M., and Lebleu, B. (2010) Cell penetrating peptides: overview and applications to the delivery of oligonucleotides. *Cell. Mol. Life Sci.* **67**, 715–726.
- (12) Vives, E., Schmidt, J., and Pelegrin, A. (2008) Cell-penetrating and cell-targeting peptides in drug delivery. *Biochim. Biophys. Acta* **1786**, 126–138.
- (13) Derossi, D., Calvet, S., Trembleau, A., Brunissen, A., Chassaing, G., and Prochiantz, A. (1996) Cell internalization of the third helix of the antennapedia homeodomain is receptor-independent. *J. Biol. Chem.* **271**, 18188–18193.
- (14) Good, L., Awasthi, S. K., Dryselius, R., Larsson, O., and Nielsen, P. E. (2001) Bactericidal antisense effects of peptide-PNA conjugates. *Nat. Biotechnol.* **19**, 360–364.
- (15) Jha, D., Mishra, R., Gottschalk, S., Wiesmüller, K.-H., Ugurbil, K., Maier, M. E., and Engelmann, J. (2011) CyLoP-1: A novel cysteine-rich cell-penetrating peptide for cytosolic delivery of cargoes. *Bioconjugate Chem.* **22**, 319–328.
- (16) Saleh, A. F., Arzumanov, A., Abes, R., Owen, D., Lebleu, B., and Gait, M. J. (2010) Synthesis and splice-redirecting activity of branched, arginine-rich peptide dendrimer conjugates of peptide nucleic acid oligonucleotides. *Bioconjugate Chem.* **21**, 1902–1911.
- (17) Vaara, M., and Porro, M. (1996) Group of peptides that act synergistically with hydrophobic antibiotics against gram-negative enteric bacteria. *Antimicrob. Agents Chemother.* **40**, 1801–1805.
- (18) Vivès, E., Brodin, P., and Lebleu, B. (1997) A truncated HIV-1 Tat protein basic domain rapidly translocates through the plasma membrane and accumulates in the cell nucleus. *J. Biol. Chem.* **272**, 16010–16017.
- (19) Lu, K., Duan, Q.-P., Ma, L., and Zhao, D.-X. (2010) Chemical strategies for the synthesis of peptide-oligonucleotide conjugates. *Bioconjugate Chem.* **21**, 187–202.
- (20) Wang, T.-P., Chiou, Y.-J., Chen, Y., Wang, E.-C., Hwang, L.-C., Chen, B.-H., Chen, Y.-H., and Ko, C.-H. (2010) Versatile phosphoramidation reactions for nucleic acid conjugations with peptides, proteins, chromophores, and biotin derivatives. *Bioconjugate Chem.* **21**, 1642–1655.
- (21) Boger, D. L., Zhou, J., Winter, B., and Kitos, P. A. (1995) Key analogs of the tetrapeptide subunit of RA-VII and deoxybouvardin. *Bioorg. Med. Chem.* **3**, 1579–1593.

- (22) Allen, V. C., Robertson, C. C., Turega, S. M., and Philp, D. (2010) A simple network of synthetic replicators can perform the logical OR operation. *Org. Lett.* *12*, 1920–1923.
- (23) Wang, T.-P., Su, Y.-C., Chen, Y., Liou, Y.-M., Lin, K.-L., Wang, E.-C., Hwang, L.-C., Wang, Y.-M., and Chen, Y.-H. (2012) In vitro selection and characterization of a novel Zn(II)-dependent phosphorothiolate thioesterase ribozyme. *Biochemistry* *51*, 496–510.
- (24) Lin, C.-M., Chiu, J.-H., Wu, I. H., Wang, B.-W., Pan, C.-M., and Chen, Y.-H. (2010) Ferulic acid augments angiogenesis via VEGF, PDGF and HIF-1 α . *J. Nutr. Biochem.* *21*, 627–633.
- (25) Proudnikov, D., and Mirzabekov, A. (1996) Chemical methods of DNA and RNA fluorescent labeling. *Nucleic Acids Res.* *24*, 4535–4542.
- (26) Grauer, A., Riechers, A., Ritter, S., and König, B. (2008) Synthetic receptors for the differentiation of phosphorylated peptides with nanomolar affinities. *Chem.—Eur. J.* *14*, 8922–8927.
- (27) Shchepinov, M. S., Denissenko, M. F., Smylie, K. J., Wörl, R. J., Leppin, A. L., Cantor, C. R., and Rodi, C. P. (2001) Matrix-induced fragmentation of P3'-N5' phosphoramidate-containing DNA: high-throughput MALDI-TOF analysis of genomic sequence polymorphisms. *Nucleic Acids Res.* *29*, 3864–3872.
- (28) Milligan, J. F., Groebe, D. R., Witherell, G. W., and Uhlenbeck, O. C. (1987) Oligoribonucleotide synthesis using T7 RNA polymerase and synthetic DNA templates. *Nucleic Acids Res.* *15*, 8783–8798.
- (29) Ho, N. W. Y., Duncan, R. E., and Gilham, P. T. (1981) Esterification of terminal phosphate groups in nucleic acids with sorbitol and its application to the isolation of terminal polynucleotide fragments. *Biochemistry* *20*, 64–67.
- (30) Dawson, R. M. C., Elliott, D. C., Elliott, W. H., and Jones, K. M. (1986) *Data for Biochemical Research*, 3rd ed.; Oxford Science Publication.
- (31) Hermanson, G. T. (1996) *Bioconjugate techniques*, Academic Press, San Diego, USA.